Acid-Assisted Reductive Elimination as a Route to Platinum(II) Products from Platinum(IV) Tris(pyrazolyl)borate Reagents

Stefan Reinartz, Peter S. White, Maurice Brookhart,* and Joseph L. Templeton*

Department of Chemistry, The University of North Carolina, Chapel Hill, North Carolina 27599-3290

Received May 26, 2000

A series of chiral cationic platinum(II) complexes of the type [κ^2-((Hpz*)BHpz*$_2$)Pt(R)(L)][BAr′$_4$] (R = Me, L = MeCN (**3**), ^{t}BuNC (**4**), py (**5**), CO (**6**), CH_2=CH_2 (**7**), PMe_2Ph (**8**); R = Ph, L = MeCN (**10**); pz* = 3,5-dimethylpyrazolyl, BAr′$_4$ = tetrakis(3,5-trifluoromethylphenyl)-borate) has been prepared. Protonation of Tp′$PtMe_2H$ (**1**) or Tp′$PtPh_2H$ (**2**) (Tp′ = hydridotris-(3,5-dimethylpyrazolyl)borate) occurs selectively at a pyrazole nitrogen atom and induces reductive elimination of methane or benzene. Subsequent addition of ligand, L, traps the platinum(II) intermediate and yields **3**−**8** and **10**. Addition of 2 equiv of PMe_2Ph led to the formation of *trans*-[κ^1-((Hpz*)BHpz*$_2$)Pt(Me)(PMe_2Ph)$_2$][BAr′$_4$] (**9**), a square-planar complex containing a rare monodentate protonated tris(pyrazolyl)borate ligand. Deprotonation of the pyrazolium ring (present after protonation of **1** or **2** and trapping with added ligand) led to the synthesis of neutral platinum(II) complexes of the type Tp′PtR(L) (R = Me, L = MeCN (**11**), SMe_2 (**12**), CO (**13**), CH_2=CH_2 (**14**); R = Ph, L = MeCN (**15**)). Complexes **11**, **12**, and **15** exhibit square-planar coordination with a bidentate Tp′ ligand, while complex **14** is trigonal bipyramidal. Tp′PtMe(CO) (**13**) is present in solution in both isomeric forms. X-ray structure determinations for the cationic complexes **3** and **6**−**9** and the neutral square-planar complex **12** are reported.

Introduction

Electrophilic platinum(II) complexes can activate alkane C−H bonds.[1,2] Hydridoalkylplatinum(IV) complexes, key species in C−H bond activation by platinum-(II), can be independently generated either by protonation of alkylplatinum(II) complexes[3,4] or by hydride addition to alkylplatinum(IV) complexes which contain good leaving groups.[5] The mechanism of C−H bond activation has been productively investigated by studying its microscopic reverse reaction, C−H reductive elimination, from these *formal* alkane C−H activation products. Methane elimination from hydridomethylplatinum(IV) complexes occurs readily unless a ligand, which both stabilizes the high platinum oxidation state and hinders formation of a five-coordinate intermediate necessary for reductive elimination, is present in the coordination sphere.[6] Stable octahedral hydridodimethylplatinum(IV) complexes can be prepared by protonation of platinum(II) complexes containing a κ^2-coordinated tridentate ligand capable of *fac* coordination.[4a−c] The crystal structure of [PPN][Tp′$PtMe_2$] (Tp′ = hydridotris(3,5-dimethylpyrazolyl)borate, PPN = bis-(triphenylphosphoranylidene)nitrogen(1+)), has confirmed that the Tp′ ligand coordinates in a bidentate fashion in such precursors.[2c]

Puddephatt and co-workers recently showed that the site of protonation in platinum(II) complexes containing ancillary ligands with a pendant third donor group is variable and depends on the relative basicities of metal and ligand.[7] Protonation of the square-planar [Tp′$PtMe_2$]$^-$ anion with a pendant pyrazole arm occurs exclusively

(1) Stahl, S. S.; Labinger, J. A.; Bercaw, J. E. *Angew. Chem., Int. Ed.* **1998**, *37*, 2181.

(2) (a) Johansson, L.; Ryan, O. B.; Tilset, M. *J. Am. Chem. Soc.* **1999**, *121*, 1974. (b) Periana, R. A.; Taube, D. J.; Gamble, S.; Taube, H.; Satoh, T.; Fujii, H. *Science* **1998**, *280*, 560. (c) Wick, D. D.; Goldberg, K. I. *J. Am. Chem. Soc.* **1997**, *119*, 10235. (d) Holtcamp, M. W.; Labinger, J. A.; Bercaw, J. E. *J. Am. Chem. Soc.* **1997**, *119*, 848.

(3) (a) Stahl, S. S.; Labinger, J. A.; Bercaw, J. E. *J. Am. Chem. Soc.* **1996**, *118*, 5961. (b) Stahl, S. S.; Labinger, J. A.; Bercaw, J. E. *J. Am. Chem. Soc.* **1995**, *117*, 9371. (c) Luinstra, G. A.; Wang, L.; Stahl, S. S.; Labinger, J. A.; Bercaw, J. E. *J. Organomet. Chem.* **1995**, *504*, 75. (d) Hill, G. S.; Rendina, L. M.; Puddephatt, R. J. *Organometallics* **1995**, *14*, 4966. (e) Hutson, A. C.; Lin, M.; Basickes, N.; Sen, A. *J. Organomet. Chem.* **1995**, *504*, 69. (f) Sen, A.; Lin, M.; Kao, L. C.; Hutson, A. C. *J. Am. Chem. Soc.* **1992**, *114*, 6385.

(4) (a) O'Reilly, S. A.; White, P. S.; Templeton, J. L. *J. Am. Chem. Soc.* **1996**, *118*, 5684. (b) Canty, A. J.; Dedieu, A.; Jin, H.; Milet, A.; Richmond, M. K. *Organometallics* **1996**, *15*, 2845. (c) Prokopchuk, E. M.; Jenkins, H. A.; Puddephatt, R. J. *Organometallics* **1999**, *18*, 2861. (d) De Felice, V.; De Renzi, A.; Panunzi, A.; Tesauro, D. *J. Organomet. Chem.* **1995**, *488*, C13.

(5) (a) Hill, G. S.; Puddephatt, R. J. *J. Am. Chem. Soc.* **1996**, *118*, 8745. (b) Hill, G. S.; Vittal, J. J.; Puddephatt, R. J. *Organometallics* **1997**, *16*, 1209.

(6) (a) Bartlett, K. L.; Goldberg, K. I.; Thatcher Bordon, W. *J. Am. Chem. Soc.* **2000**, *122*, 1456. (b) Crumpton, D. M.; Goldberg, K. I. *J. Am. Chem. Soc.* **2000**, *122*, 962. (c) Williams, B. S.; Holland, A. W.; Goldberg, K. I. *J. Am. Chem. Soc.* **1999**, *121*, 252. (d) Goldberg, K. I.; Yan, J. Y.; Breitung, E. M. *J. Am. Chem. Soc.* **1995**, *117*, 6889. (e) Hill, G. S.; Yap, G. P. A.; Puddephatt, R. J. *Organometallics* **1999**, *18*, 1408. (f) Hill, G. S.; Puddephatt, R. J. *Organometallics* **1998**, *17*, 1478. (g) Hill, G. S.; Puddephatt, R. J. *Organometallics* **1997**, *16*, 4522. (h) Jenkins, H. A.; Yap, G. P. A.; Puddephatt, R. J. *Organometallics* **1997**, *16*, 1946. (i) Roy, S.; Puddephatt, R. J.; Scott, J. D. *J. Chem. Soc., Dalton Trans.* **1989**, 2121. (j) Brown, M. P.; Puddephatt, R. J.; Upton, C. E. E. *J. Chem. Soc., Dalton Trans.* **1974**, 2457. (k) Fekl, U.; Zahl, A.; van Eldik, R. *Organometallics* **1999**, *18*, 4156.

(7) Hinman, J. G.; Baar, C. R.; Jennings, M. C.; Puddephatt, R. J. *Organometallics* **2000**, *19*, 563.

10.1021/om000440z CCC: $19.00
Publication on Web 08/22/2000

Scheme 1. NMR-Scale Protonation of Tp′PtMe$_2$H (1)

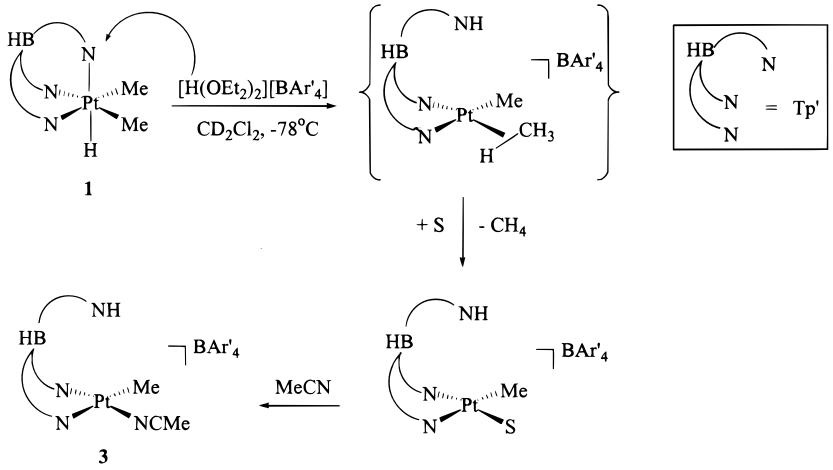

at metal to form Tp′PtMe$_2$H.[8] Decreasing the basicity of the metal center by using a less electron-donating ligand in a neutral platinum(II) complex can change the site of protonation. Protonation of TpPtMe(CO) (Tp = hydridotris(pyrazolyl)borate) occurs exclusively at the ligand, because here the pendant pyrazole nitrogen is more basic than the platinum center.[9]

The synthesis of stable hydridodialkylplatinum(IV) complexes via oxidative addition of alkanes to the [Tp′Pt^{II}Me] fragment has been demonstrated by Wick and Goldberg.[2c] The hapticity of the Tp′ ligand changes from κ^2 in the platinum(II) species to κ^3 in the platinum(IV) product, thus trapping the intermediate five-coordinate hydridodialkylplatinum(IV) species and preventing C−H reductive elimination.

The microscopic reverse of this process, namely reductive elimination of methane from Tp′PtMe$_2$H, requires high temperatures and presumably occurs from a five-coordinate intermediate generated by dissociation of one of the pyrazole rings.[10] Just as there are different possible sites for protonation in methylplatinum(II) complexes, there are three feasible sites for protonation in hydrido(dialkyl/diaryl)platinum(IV) complexes: at platinum, at the nitrogen atom of a pyrazole ligand, or at the platinum−alkyl/aryl bond. We present here results of protonation of Tp′PtMe$_2$H and Tp′PtPh$_2$H followed by the addition of trapping ligands.

Results and Discussion

NMR Spectroscopic Monitoring of the Protonation of Tp′PtMe$_2$H (1) and Tp′PtPh$_2$H (2). During our exploration of platinum(II)/platinum(IV) interconversions in bond activation processes, the conversion of Tp′PtMe$_2$H (**1**) to Tp′PtPh$_2$H (**2**) via thermolysis in benzene was investigated. In this reaction, reductive elimination of methane from **1** was thermally induced, followed by C−H activation of the solvent. In an analogous reaction, heating of Tp′PtPh$_2$H (**2**) in benzene-d_6 gave the fully deuterated species Tp′Pt(C$_6$D$_5$)$_2$D.[10] Could an alternative route be uncovered using acid reagents to induce reductive elimination of alkanes from Tp′Pt^{IV}R$_2$H under mild conditions? When the dimethyl hydride complex **1** reacts with 1 equiv of the acid [H(OEt$_2$)$_2$][BAr′$_4$][11] (BAr′$_4$ = tetrakis(3,5-trifluoromethylphenyl)borate) in CD$_2$Cl$_2$ at −78 °C, methane formation (^{1}H NMR, δ 0.14 ppm; ^{13}C NMR, δ −4.1 ppm) is observed. Both ^{1}H and ^{13}C NMR spectra show a single metal product with 1:1:1 patterns for the resonances of the Tp′ ligand, indicating a chiral metal center. An upfield resonance for the remaining platinum-bound methyl group is observed (^{1}H NMR, δ 0.39 ppm; ^{13}C NMR, δ −22.4 ppm), and a broad singlet at 11.66 ppm in the ^{1}H NMR spectrum is indicative of a protonated pyrazole ring.[12] The NMR data are consistent with the formation of [κ^2-((Hpz*)BHpz*$_2$)Pt(Me)(S)][BAr′$_4$], where S is a solvent molecule, in this case CD$_2$Cl$_2$. The platinum(II) solvento cation decomposes upon warming the sample to 0 °C, and a variety of unidentified products form. Addition of excess MeCN to the cationic intermediate at low temperatures cleanly affords the platinum(II) acetonitrile adduct [κ^2-((Hpz*)BHpz*$_2$)Pt(Me)(NCMe)][BAr′$_4$] (**3**) (vide infra).

If the dimethyl hydride **1** is treated with deuterated acid, [D(OEt$_2$)$_2$][BAr′$_4$], a broad resonance at 11 ppm is observed in the ^{2}H NMR spectrum, indicating a deuterated pyrazolium ring; *no deuterium incorporation is observed in either the remaining platinum-bound methyl group or in the evolved methane.* This implies that protonation occurs exclusively at a pyrazole nitrogen atom rather than at either the metal or a methyl site. A plausible reaction sequence is protonation of Tp′PtMe$_2$H (**1**) at a pyrazole nitrogen atom with concomitant generation of an open coordination site in a five-coordinate platinum intermediate, followed by reductive elimination of methane. Loss of methane and coordination of a solvent molecule to the three-coordinate Pt(II) species would form the square-planar solvento complex, and solvent would then be rapidly displaced by the better ligand, MeCN (Scheme 1). The proton presumably

(8) Reaction of *cis*-PtMe$_2$(SMe$_2$)$_2$ with the N-protonated ligand HTp′ leads to the formation of the platinum(IV) product Tp′PtMe$_2$H instead of the platinum(II) product (HTp′)PtMe$_2$, also indicating the greater basicity of platinum(II) relative to the free pyrazole arm.

(9) Haskel, A.; Keinan, E. *Organometallics* **1999**, *18*, 4677.

(10) (a) Jensen, M. P.; Wick, D. D.; Reinartz, S.; Templeton, J. L.; Goldberg, K. I. Manuscript in preparation. (b) Reinartz, S. Diplomarbeit, Universität Düsseldorf, 1998.

(11) Brookhart, M.; Grant, B.; Volpe, A. F., Jr. *Organometallics* **1992**, *11*, 1, 3920.

(12) (a) Ball, R. G.; Ghosh, C. K.; Hoyano, J. K.; McMaster, A. D.; Graham, W. A. G. *J. Chem. Soc., Chem. Commun.* **1989**, 341. (b) Rheingold, A. L.; Haggerty, B. S.; Trofimenko, S. *Angew. Chem., Int. Ed. Engl.* **1994**, *33*, 1983. (c) Wiley, J. S.; Oldham, W. J., Jr.; Heinekey, D. M. *Organometallics* **2000**, *19*, 1670.

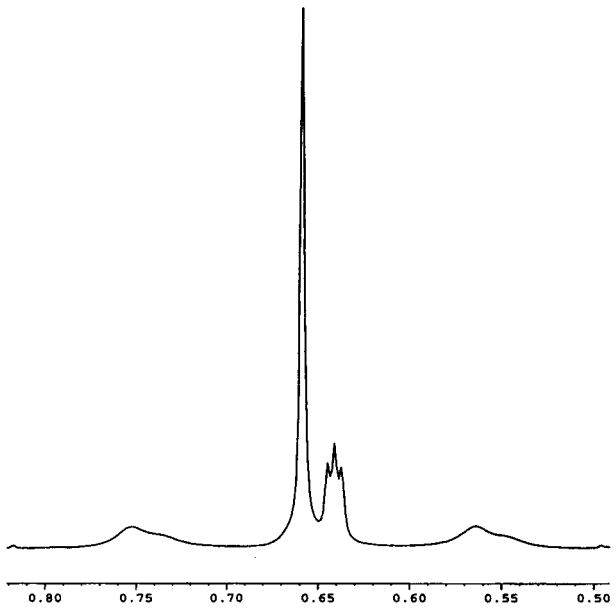

Figure 1. ^{1}H NMR (400 MHz) spectrum of the platinum-bound methyl groups of [κ^2-((Hpz*)BHpz*$_2$)Pt(CH_3/CH_2D)-(NCMe)][BAr′$_4$] (25 °C).

adds to the pyrazole ring after dechelation, but no experimental evidence is available concerning this point.

There is experimental evidence that a σ-methane complex forms as an intermediate in the protonation reaction of the dimethyl hydride **1**. When Tp′PtMe_2D (**1-*d***) reacts with 1 equiv of [H(OEt_2)$_2$][BAr′$_4$], resonances for CH_3D (1:1:1 pattern, 0.13 ppm) *and* CH_4 (s, 0.14 ppm) in about a 1:1 ratio are observed, as well as resonances for two platinum-bound methyl groups. If excess acetonitrile is added, the cationic platinum(II) acetonitrile adduct [κ^2-((Hpz*)BHpz*$_2$)Pt(Me)(NCMe)]-[BAr′$_4$] (**3**) can again be isolated. The two distinct types of platinum-bound methyl groups resonate as a singlet (Pt−CH_3) and a 1:1:1 triplet (Pt−CH_2D) (Figure 1). This pattern illustrates that deuterium scrambles from the hydride position into the methyl position and implicates reversible formation of a σ-methane intermediate prior to methane dissociation (Scheme 2). The broadening of the platinum satellites at room temperature and their disappearance at low temperature is caused by spin relaxation by chemical shift anisotropy.[13]

The protonation of Tp′PtPh_2H was also monitored by NMR spectroscopy. In this case free benzene (s, 7.33 ppm) and the solvento cation [κ^2-((Hpz*)BHpz*$_2$)Pt(Ph)-(S)][BAr′$_4$] are observed (for numerical NMR data see the Experimental Section). This solvento species can be trapped with MeCN. Encouraged by these NMR results, we performed the protonation reactions on a larger scale and with a variety of trapping ligands.

Synthesis of [κ^2-((Hpz*)BHpz*$_2$)Pt(Me)(L)][BAr′$_4$] (L = MeCN (3), ^{t}BuNC (4), py (5), CO (6), CH_2=CH_2 (7)). The cationic platinum(II) complexes **3**−**7** were synthesized by protonation of Tp′PtMe_2H (**1**) with [H(OEt_2)$_2$][BAr′$_4$] in CH_2Cl_2 at −78 °C and subsequent addition of the trapping ligand, L (Scheme 3). After recrystallization, **3**−**7** were obtained in good yields as colorless, air-stable crystals.

The ^{1}H NMR spectrum of [κ^2-((Hpz*)BHpz*$_2$)Pt(CH_3)-(NCMe)][BAr′$_4$] (**3**) in CD_2Cl_2 displays the N−*H* resonance of the protonated pyrazole ring at 12.22 ppm. The protons of the platinum-bound methyl group resonate at 0.66 ppm with two-bond coupling to platinum of 76 Hz (^{195}Pt, 33.4% abundant), while the carbon atom of the methyl group appears at −21.5 ppm in the ^{13}C{^{1}H} NMR spectrum with one-bond coupling to platinum of 641 Hz. The carbon atoms of the coordinated acetonitrile molecule resonate in the expected regions of 116.7 ppm (N*C*CH_3) and 4.1 ppm (NC*C*H_3).[14] NMR data for analogous resonances of the cationic complexes **3**−**9** are summarized in Table 1.[15]

The N−*H* resonances for the cationic methylplatinum(II) complexes **3**−**9** cover a chemical shift range of about 4 ppm, from 9.76 to 13.81 ppm. The protons of the platinum-bound methyl group resonate between 0.24 and 0.82 ppm, while the two-bond coupling to platinum varies only slightly from 72 to 76 Hz. The carbon atom of the platinum-bound methyl group resonates well upfield in a chemical shift range between −13.5 and −23.7 ppm, and differences of up to 200 Hz are observed for the one-bond coupling to platinum. $^1J_{Pt-C}$ is smallest for the methyl group in the methyl carbonyl complex **6** (523 Hz), while it is largest for the methyl pyridine complex **5** (725 Hz).

The ^{1}H NMR resonance for the *tert*-butyl isocyanide ligand in [κ^2-((Hpz*)BHpz*$_2$)Pt(Me)(CN^{t}Bu)][BAr′$_4$] (**4**) is seen at 1.46 ppm. The carbon atoms of the coordinated ^{t}BuNC molecule display signals at 59.2 ppm (*C*(CH_3)$_3$) and 30.2 ppm (C(*C*H_3)$_3$). The resonance of the isocyanide carbon atom was not located.

The ^{1}H NMR spectrum of [κ^2-((Hpz*)BHpz*$_2$)Pt(Me)(py)][BAr′$_4$] (**5**) shows the N−*H* resonance at 13.81 ppm, which is further downfield than in the other cationic complexes reported here. Diagnostic ^{1}H NMR signals are observed for the protons of the coordinated pyridine molecule (H_{ortho}, 8.35 ppm, d of d, $^3J_{H-H}$ = 6.4 Hz, $^4J_{H-H}$ = 1.5 Hz, $^3J_{Pt-H}$ = 44 Hz; H_{para}, 7.85 ppm, t of t, $^3J_{H-H}$ = 7.6 Hz, $^4J_{H-H}$ = 1.5 Hz; H_{meta}, 7.32 ppm, d of d, $^3J_{H-H}$ = 7.6 Hz, $^3J_{H-H}$ = 6.4 Hz). The resonance for the ortho carbons of the pyridine ligand is observed at 127.2 ppm ($^2J_{Pt-C}$ = 46 Hz).

The solid-state IR spectrum of the cationic monocarbonyl complex [κ^2-((Hpz*)BHpz*$_2$)Pt(Me)(CO)][BAr′$_4$] (**6**) shows an absorption at 2099 cm^{-1} for the CO stretch, indicating only weak back-donation from the highly electrophilic platinum(II) center into the CO(π*) orbital.[16] An IR absorption at 2518 cm^{-1} is observed for the B−H stretch of the Tp′ ligand. The carbon atom of

(13) (a) Benn, R.; Büch, H. M.; Reinhardt, R.-D. *Magn. Reson. Chem.* **1985**, *23*, 559. (b) Lallemand, J.-Y.; Soulié, J.; Chottard, J.-C. *J. Chem. Soc., Chem. Commun.* **1980**, 436. (c) Dechter, J. D.; Kowalewski, J. *J. Magn. Reson.* **1984**, *59*, 146. (d) Doddrell, D. M.; Barron, P. F.; Clegg, D. E.; Bowie, C. *J. Chem. Soc., Chem. Commun.* **1982**, 575. (e) For a recent reference dealing with TpTl complexes, see: Ghosh, P.; Desrosiers, P. J.; Parkin, G. *J. Am. Chem. Soc.* **1998**, *120*, 10416.

(14) See e.g.: (a) Brookhart, M.; Rix, F. C.; DeSimone, J. M.; Barborak, J. C. *J. Am. Chem. Soc.* **1992**, *114*, 5894. (b) Johansson, L.; Ryan, O. B.; Rømming, C.; Tilset, M. *Organometallics* **1998**, *17*, 3957.

(15) The syntheses of water and tetrahydrofuran adducts analogous to the acetonitrile adduct **3** were attempted. The ^{1}H NMR spectrum of the crude reaction product, when water or THF was used as trapping ligand after protonation of Tp′PtMe_2H (**1**), showed resonances indicative of the desired compounds, but attempts to purify the products by recrystallization led to decomposition. [(HTp′)PtMe(OH_2)][BAr′$_4$]: δ 13.64 (1H, N*H*), 4.85 (br, 2H, H_2O), 0.75 (s, 3H, $^2J_{Pt-H}$ = 70 Hz, Pt−CH_3). [(HTp′)PtMe(THF)][BAr′$_4$]: δ 12.57 (1H, N*H*), 3.77, 1.89 (m, 8H, Pt−*THF*), 0.71 (s, 3H, $^2J_{Pt-H}$ = 70 Hz, Pt−CH_3).

Scheme 2. Isotope Scrambling in the Protonation of Tp′PtMe$_2$D (1-*d*)

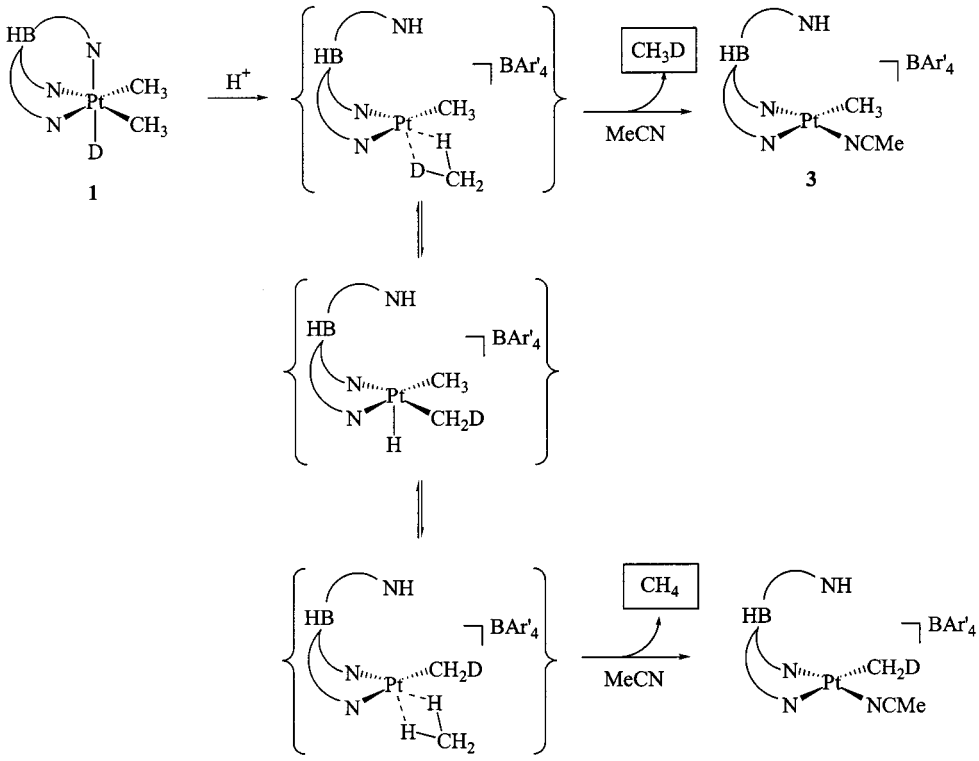

Scheme 3. Synthesis of [κ^2-((Hpz*)BHpz*$_2$)Pt(Me)(L)][BAr′$_4$] (L = MeCN (3), ^{t}BuNC (4), py (5), Co (6), CH$_2$≡CH$_2$ (7)) via Protonation of Tp′Pt(CH$_3$)$_2$H (1)

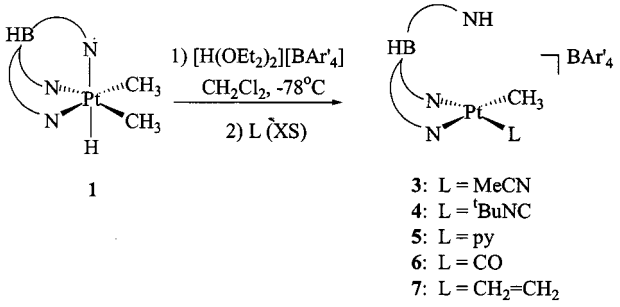

Table 1. Selected NMR Data for Complexes 3−9

complex	δ(N−*H*)/ ppm	δ(Pt−C*H*$_3$)/ ppm	$^2J_{Pt-H}$/ Hz	δ(Pt−CH$_3$)/ ppm	$^1J_{Pt-C}$/ Hz
3	12.22	0.66	76	−21.5	641
4	10.76	0.60	76	−23.4	589
5	13.81	0.81	76	−16.1	725
6	11.29	0.82	73	−19.9	523
7	9.76	0.24	72	−13.5	632
8	10.42	0.45	72	−19.3	642
9	11.74	0.32	72	−20.1	613

the platinum-bound carbon monoxide resonates relatively far upfield at 164.0 ppm in the ^{13}C NMR spectrum. If ^{13}C-labeled CO is used in the synthesis of **6**, the platinum satellites of this resonance can be easily detected, yielding a one-bond coupling to platinum of 1877 Hz. The CO stretching frequency of ^{13}CO-labeled **6** at 2049 cm^{-1} in the solid-state IR spectrum is close to the harmonic oscillator prediction of 2052 cm^{-1}.

The N−*H* resonance of [κ^2-((Hpz*)BHpz*$_2$)Pt(Me)-(CH$_2$=CH$_2$)][BAr′$_4$] (**7**) appears at 9.76 ppm in the ^{1}H NMR spectrum, which is further upfield than in the other complexes reported in this paper. A complex second-order pattern is obtained for the four protons of the coordinated ethylene molecule. Multiplets with broad platinum satellites (J_{Pt-H} = 69 Hz, 2 H each) are observed at 3.88 and 3.69 ppm for this chiral complex, indicating rapid rotation of the ethylene ligand about the midpoint of the ethylene−platinum bond on the NMR time scale at room temperature. This conclusion is reinforced by the presence of only a single ^{13}C resonance for both ethylene carbons at 69.5 ppm ($^1J_{Pt-C}$ = 200 Hz). A barrier of 7 kcal/mol was calculated for ethylene rotation on the basis of variable-temperature NMR studies (at T_c = 156 K).

Similar NMR features have been reported for other platinum(II) ethylene complexes.[17] The cationic platinum(II) diimine compounds reported by Ruffo and coworkers are of particular interest here, because the protonated Tp′ ligand in complex **7** effectively acts as a neutral, bidentate nitrogen donor ligand. Unlike complex **7**, Ruffo's methylplatinum(II) ethylene complexes are prochiral rather than chiral; therefore, only one set of proton resonances is observed in the ^{1}H NMR spectrum for the platinum-bound ethylene molecule. The ethylene protons of [PtMe(daproph)(ethylene)][BF$_4$] (daproph = diacetyl bis(2,6-isopropylphenylimine), for example, appear at 3.72 ppm, while the ethylene carbon atoms resonate at 73.8 ppm ($^1J_{Pt-C}$ = 192 Hz).[17a] These data are nearly identical with those for complex **7**.

(16) (a) Baar, C. R.; Jennings, M. C.; Puddephatt, R. J.; Muir, K. W. *Organometallics* **1999**, *18*, 4373. (b) De Felice, V.; De Renzi, A.; Ferrara, M. L.; Panunzi, A. *J. Organomet. Chem.* **1996**, *513*, 97. (c) Andreini, B. P.; Dell'Amico, D. B.; Calderazzo, F.; Venturi, M. G.; Pelizzi, G.; Segre, A. *J. Organomet. Chem.* **1988**, *354*, 357. (d) Irving, R. J.; Magnusson, E. A. *J. Chem. Soc.* **1956**, 1860.

(17) (a) Fusto, M.; Giordano, F.; Orabona, I.; Ruffo, F.; Panunzi, A. *Organometallics* **1997**, *16*, 5981. (b) Ganis, P.; Orabona, I.; Ruffo, F.; Vitagliano, A. *Organometallics* **1998**, *17*, 2646. (c) Scott, J. D.; Puddephatt, R. J. *J. Chem. Soc., Chem. Commun.* **1984**, 193.

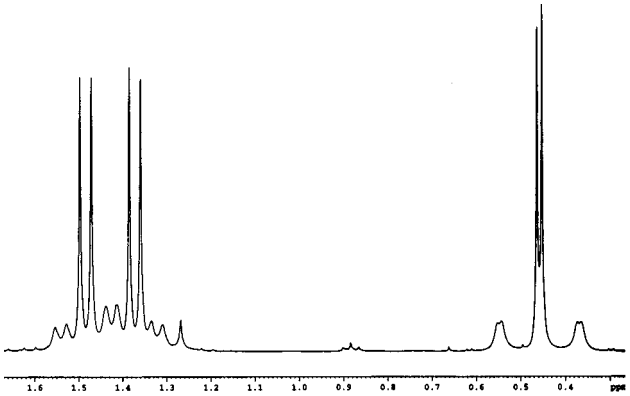

Figure 2. ^{1}H NMR (400 MHz) spectrum of **8**, methyl region.

Scheme 4. Synthesis of Complexes 8 and 9: Formation of κ^1-(HTp′)

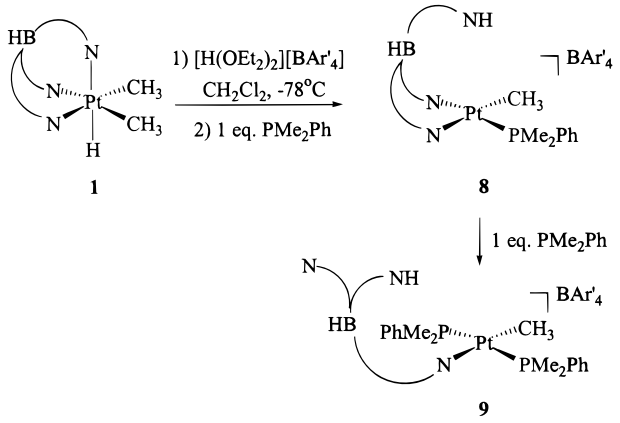

PMe$_2$Ph as Trapping Ligand: Observation of Monodentate (Hpz*)BHpz*$_2$. If *1 equiv* of PMe$_2$Ph is used as a trapping ligand after protonation of Tp′PtMe$_2$H (**1**) with [H(OEt$_2$)$_2$][BAr′$_4$], a simple square-planar platinum(II) phosphine adduct analogous to the other complexes forms. Recrystallization of the crude reaction product yields [κ^2-((Hpz*)BHpz*$_2$)Pt(Me)(PMe$_2$Ph)][BAr′$_4$] (**8**). The ^{1}H NMR spectrum of **8** displays a set of high-field methyl signals due to the platinum-bound methyl group (0.45 ppm with $^3J_{P-H}$ = 4.9 Hz and $^2J_{Pt-H}$ = 72 Hz) and the diastereotopic methyl groups of the phosphine ligand (1.48 and 1.37 ppm with $^2J_{P-H}$ = 10.3 Hz and $^3J_{Pt-H}$ = 45 Hz). The platinum satellites of the PMe$_2$Ph methyl resonances overlap, so that only six of the eight possible signals are seen (Figure 2). The ^{31}P signal of **8** (17.9 ppm) shows large coupling to platinum ($^1J_{Pt-P}$ = 4114 Hz), as is typical for a phosphine *trans* to a nitrogen donor ligand, here a pyrazolyl group.[18]

If *2 equiv* of the PMe$_2$Ph is added following acid addition to Tp′PtMe$_2$H (**1**), the bisphosphine complex *trans*-[κ^1-((Hpz*)BHpz*$_2$)Pt(Me)(PMe$_2$Ph)$_2$][BAr′$_4$] (**9**) forms (Scheme 4). Only one ^{31}P signal for the platinum-bound phosphine ligands is present (0.87 ppm) with a considerably smaller one-bond coupling to platinum of 2942 Hz, which is in accord with a *trans* arrangement of the two phosphines.[18] Further support for this *trans* arrangement comes from the ^{1}H NMR spectrum of **9**. The platinum-bound methyl group appears as a triplet ($^3J_{P-H}$ = 7.3 Hz) at 0.35 ppm with platinum coupling of 72 Hz. The resonances of the tris(pyrazolyl)borate ligand display the 2:1 pattern indicative of a mirror plane in the molecule. On the basis of these NMR data the structure of **9** can be assigned as a cationic square-planar complex with two PMe$_2$Ph ligands *trans* to each other and a methyl ligand *trans* to a *monodentate* (Hpz*)BHpz*$_2$.

Scheme 5. Synthesis of [κ^2-((Hpz*)BHpz*$_2$)Pt(Ph)(NCMe)][BAr′$_4$] (10)

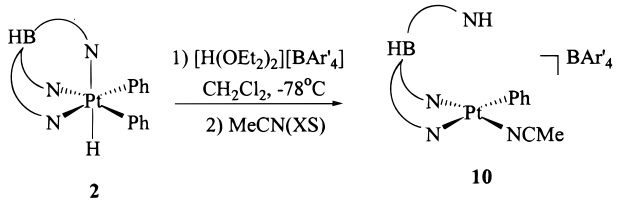

The mirror plane in the molecule relates the two phosphine ligands to one another, but the two methyl groups on each phosphine remain diastereotopic. Indeed, the ^{1}H NMR spectrum reveals pseudo triplets at 1.52 and 1.12 ppm ($^2J_{P-H}$ = 3.4 Hz, $^3J_{Pt-H}$ = 30 Hz) for the diastereotopic methyl groups.

The unusual κ^1 coordination mode of the protonated Tp′ ligand in **9** is analogous to the observed κ^1 coordination mode of the unprotonated Tp′ ligand. Etienne[19a] and, more recently, Carmona[19b] have both reported the stepwise displacement from κ^3 to κ^2 to κ^1 of coordinated pyrazole rings by phosphine ligands, and Carmona has completely severed all three metal−nitrogen bonds and used Tp′ as an uncoordinated counterion.[19b]

Synthesis of [κ^2-((Hpz*)BHpz*$_2$)Pt(Ph)(NCMe)][BAr′$_4$] (10). On the basis of the low-temperature protonation results with Tp′PtPh$_2$H (**2**), the synthesis of **10** via protonation of the diphenyl hydride **2** and trapping with excess acetonitrile was performed on a larger scale. Recrystallization of the crude product from diethyl ether/pentanes yielded **10** as light yellow, air-stable crystals (Scheme 5).

The ^{1}H NMR spectrum of the platinum(II) product **10** shows the N−*H* resonance at 12.38 ppm. The phenyl ring is rotating rapidly on the NMR time scale, since the *ortho* protons appear as a single resonance at 6.82 ppm ($^3J_{Pt-H}$ = 44 Hz); the *para* and *meta* protons overlap in a multiplet at 6.95 ppm. The ^{13}C NMR spectrum exhibits resonances of the coordinated acetonitrile molecule at 117.5 ppm (N*C*CH$_3$) and 4.2 ppm (NC*C*H$_3$).[14]

X-ray Structures of [κ^2-((Hpz*)BHpz*$_2$)Pt(Me)(L)][BAr′$_4$] (L = MeCN (3), CO (6), CH$_2$=CH$_2$ (7), PMe$_2$Ph (8)) and [κ^1-((Hpz*)BHpz*$_2$)Pt(Me)(PMe$_2$Ph)$_2$][BAr′$_4$] (9). The structural features of these cationic platinum(II) complexes containing a protonated Tp′ ligand were investigated in the solid state. An ORTEP diagram of [κ^2-((Hpz*)BHpz*$_2$)Pt(Me)(NCMe)][BAr′$_4$] (**3**) is shown in Figure 3. Most noticeable is the fact that the Tp′ ligand retains the propeller disposition

(18) (a) Pidcock, A.; Richards, R. E.; Venanzi, L. M. *J. Chem. Soc. A* **1966**, 1707. (b) Kennedy, J. D.; McFarlane, W.; Puddephatt, R. J.; Thompson, P. J. *J. Chem. Soc., Dalton Trans.* **1976**, 874.

(19) (a) Malbosc, F.; Kalck, P.; Daran, J.-C.; Etienne, J. *J. Chem. Soc., Dalton Trans.* **1999**, 271. (b) Paneque, M.; Sirol, S.; Trujillo, M.; Gutierrez-Puebla, E.; Monge, M. A.; Carmona, E. *Angew. Chem., Int. Ed.* **2000**, *39*, 218.

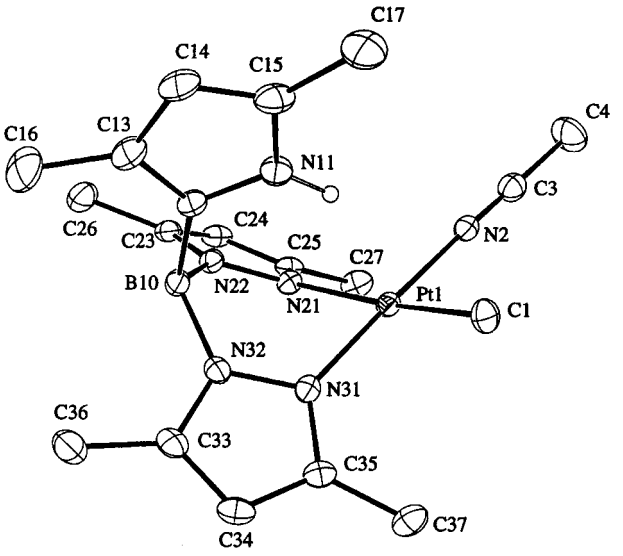

Figure 3. ORTEP diagram of [κ^2-((Hpz*)BHpz*$_2$)Pt(CH$_3$)(NCMe)][BAr′$_4$] (**3**). Ellipsoids are drawn with 50% probability; the BAr′$_4$ counterion is omitted for clarity.

Table 2. Selected Bond Distances (Å) and Angles (deg) for Complex 3

Pt1−C1	2.037(5)	Pt1−N31	1.987(4)
Pt1−N2	1.969(4)	Pt1−H11	2.325
Pt1−N21	2.120(4)	N11−H11	0.960(4)
C1−Pt1−N2	85.95(20)	N2−Pt1−N21	94.87(16)
C1−Pt1−N21	172.77(19)	N2−Pt1−N31	177.96(16)
C1−Pt1−N31	92.47(19)	N21−Pt1−N31	86.86(15)
C1−Pt1−H11	83.64(16)		

of the nitrogen heterocycles, thus leaving the protonated pyrazole nitrogen atom above the square plane. The hydrogen bound to the pyrazole nitrogen atom, which was located in the difference Fourier map, has been placed in a calculated position, and it is located within bonding distance to platinum (2.325 Å; Table 2), consistent with a three-center−four-electron N−H−Pt bond.[20] Only in the structure of this acetonitrile adduct among the five cations that were structurally characterized is this peculiarity observed. Reflecting the strong *trans* influence of the methyl group, the Pt1−N21 distance *trans* to the methyl ligand of 2.120(3) Å is significantly longer (0.13 Å) than the Pt−N31 distance of 1.987(4) Å *trans* to the acetonitrile ligand.

An ORTEP diagram of [κ^2-((Hpz*)BHpz*$_2$)Pt(CH$_3$)(CO)][BAr′$_4$] (**6**) is shown in Figure 4. The structure closely resembles the recently reported structure of [κ^2-((Hpz)BHpz$_2$)Pt(CH$_3$)(CO)][BF$_4$] in that the protonated pyrazole nitrogen atom is turned away from the platinum square plane.[9] The Pt−N distance *trans* to the methyl ligand of 2.092(5) Å (Table 3) is slightly longer than the Pt−N distance *trans* to the CO ligand of 2.074(5) Å. These bond lengths are similar to the bond lengths reported for [[κ^2-(Hpz)BH(pz)$_2$]Pt(CH$_3$)(CO)][BF$_4$]: Pt−N(*trans* to methyl) = 2.075 Å, Pt−N(*trans* to CO) = 2.050 Å. Evidently the 3,5-dimethylpyrazole has little influence on the geometry relative to the parent pyrazole analogue.

(20) (a) Brammer, L.; Zhao, D.; Ladipo, F. L.; Braddock-Wilking, J. *Acta Crystallogr.* **1995**, *B51*, 632. (b) Albinati, A.; Lianza, F.; Pregosin, P. S.; Müller, B. *Inorg. Chem.* **1994**, *33*, 2522. (c) Wehman-Ooyevaar, I. C. M.; Grove, D. M.; Kooijman, H.; van der Sluis, P.; Spek, A. L.; van Koten, G. *J. Am. Chem. Soc.* **1992**, *114*, 9916.

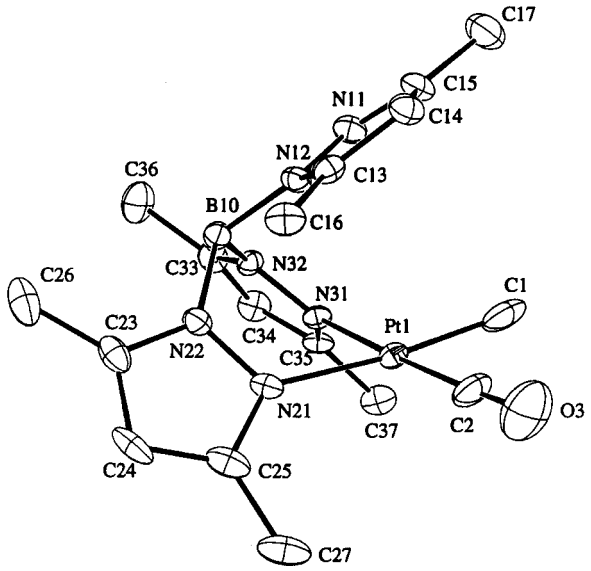

Figure 4. ORTEP diagram of [κ^2-((Hpz*)BHpz*$_2$)Pt(CH$_3$)(CO)][BAr′$_4$] (**6**). Ellipsoids are drawn with 50% probability; the BAr′$_4$ counterion is omitted for clarity.

Table 3. Selected Bond Distances (Å) and Angles (deg) for Complex 6

Pt1−C1	2.061(10)	Pt1−N31	2.074(5)
Pt1−C2	1.868(8)	C2−O3	1.094(11)
Pt1−N21	2.092(5)		
C1−Pt1−C2	88.2(3)	C2−Pt1−N31	178.1(3)
C1−Pt1−N21	173.1(3)	N21−Pt1−N31	83.94(21)
C1−Pt1−N31	90.4(3)	Pt1−C2−O3	175.8(8)
C2−Pt1−N21	97.4(3)		

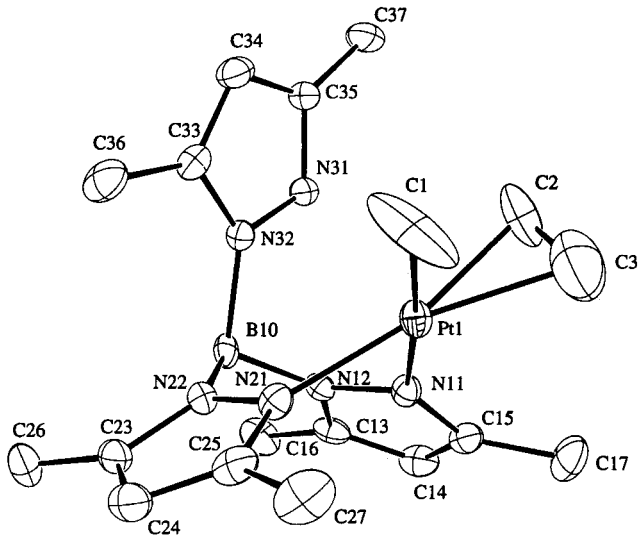

Figure 5. ORTEP diagram of [κ^2-((Hpz*)BHpz*$_2$)Pt(CH$_3$)(CH$_2$=CH$_2$)][BAr′$_4$] (**7**). Ellipsoids are drawn with 50% probability; the BAr′$_4$ counterion is omitted for clarity.

An ORTEP diagram of [κ^2-((Hpz*)BHpz*$_2$)Pt(CH$_3$)(CH$_2$=CH$_2$)][BAr′$_4$] (**7**) is shown in Figure 5. The protonated pyrazole nitrogen atom is turned away from the platinum square plane as in CO adduct **6**. The Pt−N distance *trans* to the methyl ligand of 2.101(3) Å (Table 4) is slightly longer than the Pt−N distance *trans* to the ethylene ligand of 2.085(3) Å. As expected, the ethylene ligand is oriented approximately perpendicular to the platinum square plane (tilt angle 74.5°).[21] Unfavorable steric interactions between the ethylene ligand

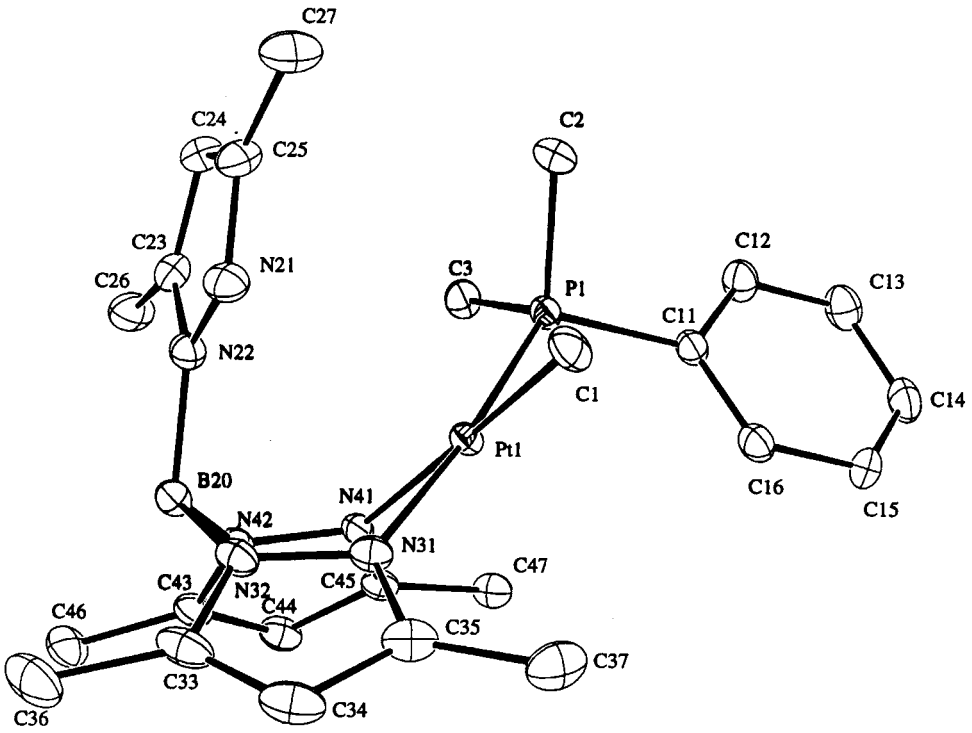

Figure 6. ORTEP diagram of [κ^2-((Hpz*)BHpz*$_2$)Pt(CH$_3$)(PMe$_2$Ph)][BAr′$_4$] (**8**). Ellipsoids are drawn with 50% probability; the BAr′$_4$ counterion is omitted for clarity.

Table 4. Selected Bond Distances (Å) and Angles (deg) for Complex 7

Pt1−C1	2.048(4)	Pt1−N11	2.101(3)
Pt1−C2	2.114(6)	Pt1−N21	2.085(3)
Pt1−C3	2.171(8)	C2−C3	1.181(14)
C1−Pt1−C2	90.43(24)	C2−Pt1−N21	164.14(21)
C1−Pt1−N11	174.7(3)	C3−Pt1−N11	99.30(24)
C1−Pt1−N21	92.11(19)	N11−Pt1−N21	85.54 (11)
C2−Pt1−C3	32.0(4)	Pt1−C2−C3	76.7(5)
C2−Pt1−N11	90.57(19)	Pt1−C3−C2	71.3(5)

Table 5. Selected Bond Distances (Å) and Angles (deg) for Complex 8

Pt1−P1	2.220(1)	Pt1−N31	2.096(3)
Pt1−C1	2.060(4)	Pt1−N41	2.125(3)
P1−Pt1−C1	88.22(13)	C1−Pt1−N41	174.23(15)
P1−Pt1−N31	173.77(9)	N31−Pt1−N41	84.81(12)
P1−Pt1−N41	97.15(8)	Pt1−P1−C11	115.48(13)
C1−Pt1−N31	89.63(15)		

and either the protonated pyrazole ring or the proximal methyl group of the *cis* pyrazole ring may prevent perfect vertical alignment of the olefin relative to the square plane.

The ORTEP diagram of [κ^2-((Hpz*)BHpz*$_2$)Pt(CH$_3$)(PMe$_2$Ph)][BAr′$_4$] (**8**) shown in Figure 6 illustrates that the protonated pyrazole nitrogen atom is turned away from the platinum square plane, as is also observed in **6** and **7**. The Pt−N distance *trans* to the methyl ligand of 2.125(3) Å (Table 5) is slightly longer than the Pt−N distance *trans* to the phosphine ligand of 2.096(3) Å, indicating that the methyl group exerts a stronger *trans* influence than the PMe$_2$Ph ligand. The phenyl group on the phosphine ligand is located away from the protonated pyrazole ring in order to minimize steric interactions.

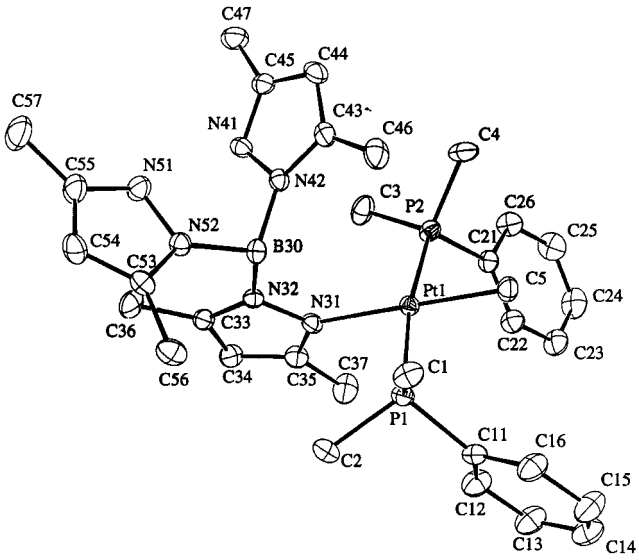

Figure 7. ORTEP diagram of [κ^1-((Hpz*)BHpz*$_2$)Pt(CH$_3$)-(PMe$_2$Ph)$_2$][BAr′$_4$] (**9**). Ellipsoids are drawn with 50% probability; the BAr′$_4$ counterion is omitted for clarity.

An ORTEP diagram of the cationic bisphosphine complex [κ^1-((Hpz*)BHpz*$_2$)Pt(CH$_3$)(PMe$_2$Ph)$_2$][BAr′$_4$] (**9**) is shown in Figure 7. The solid-state structure confirms the coordination sphere suggested by NMR data: complex **9** indeed contains a monodentate, protonated Tp′ ligand, one methyl ligand, and two phosphine ligands *trans* to each other in a square-planar platinum(II) coordination sphere. The Pt−P distances (2.286(1) and 2.295(1) Å; Table 6) and Pt−CH$_3$ distance of 2.059(4) Å do not change significantly from the

(21) For crystal structures of square-planar platinum(II) ethylene complexes see e.g.: (a) Baar, C. R.; Jenkins, H. A.; Yap, G. P. A.; Puddephatt, R. J. *Organometallics* **1998**, *17*, 4330. (b) Jarvis, J. A. J.; Kilbourn, B. T.; Owston, P. G. *Acta Crystallogr.* **1971**, *B27*, 366. (c) Bokii, G. B.; Kukina, G. A. *Akad. Nauk SSSR Kristallogr.* **1957**, *2*, 400. (d) Alderman, P. R. H.; Owston, P. G.; Rowe, J. M. *Acta Crystallogr.* **1960**, *13*, 149.

Table 6. Selected Bond Distances (Å) and Angles (deg) for Complex 9

Pt1−P1	2.286(1)	Pt1−C5	2.059(4)
Pt1−P2	2.295(1)	Pt1−N31	2.113(3)
P1−Pt1−P2	170.46(4)	P2−Pt1−C5	88.40(11)
P1−Pt1−C5	86.50(11)	P2−Pt1−N31	93.09(9)
P1−Pt1−N31	92.08(9)	C5−Pt1−N31	178.44(14)

Scheme 6. Synthesis of Tp′Pt^{II} Complexes via a Protonation/Deprotonation Route

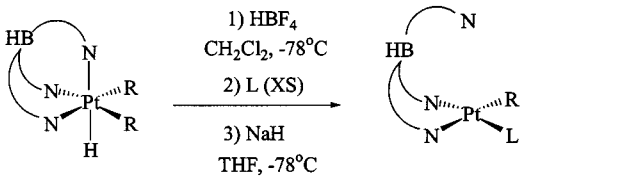

1: R = Me
2: R = Ph

11: R = Me, L = MeCN
12: R = Me, L = SMe_2
13: R = Me, L = CO
14: R = Me, L = CH_2=CH_2
15: R = Ph, L = MeCN

monophosphine complex **8**. As in **8**, the phenyl groups on the phosphine ligands reside on the opposite side of the platinum square plane away from the two pyrazole rings in order to minimize steric interactions.

Synthesis of Neutral Tp′Pt^{II} Complexes via a Protonation/Deprotonation Route. NMR experiments provided evidence that the cationic Pt(II) complexes **3** (MeCN), **6** (CO), and **7** (CH_2=CH_2) reacted with a variety of bases (NaH, KO^{t}Bu, LDA) to form neutral Tp′PtMe(L) (L = MeCN, CO, CH_2=CH_2) complexes by deprotonation of the protonated pyrazole ring. Attempts to purify these complexes were complicated by the high solubility of contaminating BAr'_4 salts, which form as side products. Would the use of a different counterion, for example $[BF_4]^-$ or $[OTf]^-$, be advantageous in removing the salt byproducts? Protonation of the dimethyl hydride complex **1** with triflic acid led to decomposition rather than the desired platinum(II) products, but protonation with tetrafluoroboric acid and trapping with MeCN yielded [κ^2-((Hpz*)BHpz*$_2$)Pt(CH$_3$)(NCMe)][BF_4] (**3a**).

Given the clean formation of [κ^2-((Hpz*)BHpz*$_2$)Pt(CH$_3$)(NCMe)][BF_4] (**3a**), the dimethyl hydride **1** was protonated with HBF_4 prior to trapping with added ligand, and a series of cationic platinum(II) intermediates of the form [κ^2-((Hpz*)BHpz*$_2$)Pt(CH$_3$)(L)][BF_4] (L = MeCN, CO, CH_2=CH_2, SMe_2) was generated in solution but not purified. Solvent exchange by removal of CH_2Cl_2 and addition of THF was followed by addition of NaH; purification of the resulting neutral products was accomplished by chromatography. The neutral Tp′Pt^{II} complexes **11**−**15** were isolated in analytically pure form as white solids (Scheme 6).

The ^{1}H NMR spectrum of Tp′PtMe(NCMe) (**11**) displays resonances for three unique pyrazole rings, indicating a chiral metal center. The protons of the platinum-bound methyl group resonate at 0.38 ppm ($^2J_{Pt-H}$ = 77 Hz). The ^{13}C{^{1}H} NMR spectrum shows characteristic signals at −23.7 ppm ($^1J_{Pt-C}$ = 668 Hz, Pt−*C*H$_3$), 114.9 ppm (N*C*CH$_3$), and 4.2 ppm (NC*C*H$_3$). The solid-state IR spectrum of **11** displays an absorption at 2459 cm^{-1} (2478 cm^{-1} in CH_2Cl_2) for the B−H stretch of the Tp′ ligand, indicating a κ^2 coordination mode.[22] The square-planar structural assignment for **11** with a bidentate Tp′ ligand in solution is supported by the ^{11}B NMR chemical shift of −6.12 ppm. ^{11}B NMR is a convenient method to determine the coordination mode of hydridotris(3,5-dimethylpyrazolyl)borate.[23] Chemical shifts near −6 ppm are seen for complexes in which the ligand coordinates in a bidentate fashion; chemical shifts of −8.5 ppm or higher are observed in complexes with a tridentate Tp′ ligand. Table 7 shows the ^{11}B chemical shifts for the neutral platinum(II) complexes **11**−**14** and for the dimethyl hydride **1**. The ^{11}B NMR data agree with the conclusions drawn from the BH stretching frequencies concerning the coordination mode of the Tp′ ligand.

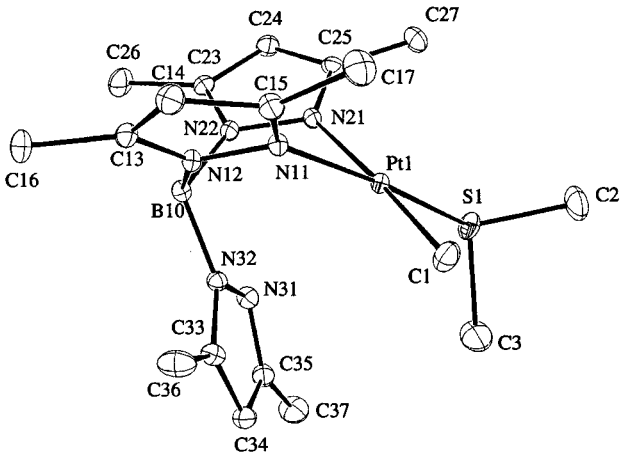

Figure 8. ORTEP diagram of Tp′PtMe(SMe_2) (**12**). Ellipsoids are drawn with 50% probability.

Table 7. ^{11}B NMR Data for Complexes 1 and 11−14

complex	δ(*B*−H)/ppm	coordination mode
1	−8.63	κ^3
11	−6.12	κ^2
12	−6.01	κ^2
13	−7.38	average between κ^2 and κ^3 (see text)
14	−8.72	κ^3

The spectroscopic features of Tp′PtMe(SMe_2) (**12**) are almost identical with those of **11**, although the dimethyl sulfide complex **12** is fluxional at room temperature. At 243 K, the ^{1}H NMR spectrum indicates a chiral metal center. The diastereotopic methyl groups of the SMe_2 ligand resonate at 2.09 ppm ($^3J_{Pt-H}$ = 57 Hz) and 1.93 ppm ($^3J_{Pt-H}$ = 51 Hz), and the protons of the platinum-bound methyl group appear at 0.23 ppm ($^2J_{Pt-H}$ = 75 Hz). The IR spectrum of **12** shows an absorption at 2455 cm^{-1} (KBr) or 2474 cm^{-1} (CH_2Cl_2) for the B−H stretch of the Tp′ ligand, and a signal at −6.12 ppm is observed in the ^{11}B NMR, all indicating κ^2 coordination.

The structural features of one neutral platinum(II) complex containing a bidentate Tp′ ligand have been investigated. An ORTEP diagram of Tp′PtMe(SMe_2) (**12**) is shown in Figure 8. Most noticeable is the fact that the Tp′ ligand indeed coordinates to the metal center in a bidentate fashion. The Pt−N bond *trans* to methyl (2.115(2) Å; Table 8) is longer than the Pt−N distance *trans* to the SMe_2 ligand (2.039(2) Å), and the uncoordinated pyrazole ring is rotated away from the platinum(II) square plane.

(22) Akita, M.; Ohta, K.; Takahashi, Y.; Hikichi, S.; Moro-oka, Y. *Organometallics* **1997**, *16*, 4121.
(23) Northcutt, T. O.; Lachiotte, R. J.; Jones, W. D. *Organometallics* **1998**, *17*, 5148.

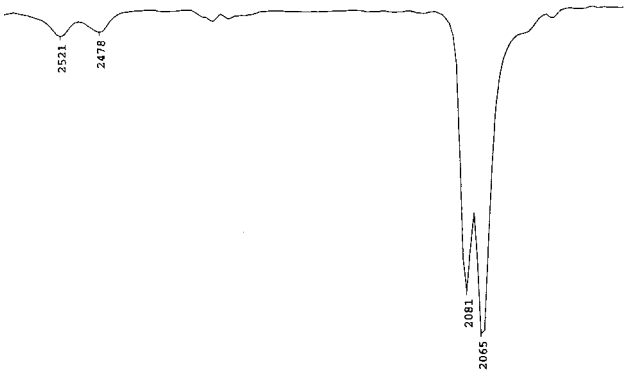

Figure 9. Solution IR spectrum (hexanes) of Tp′PtMe(CO) (**13**).

Table 8. Selected Bond Distances (Å) and Angles (deg) for Complex 12

Pt1−S1	2.2495(7)	Pt1−N21	2.115(2)
Pt1−C1	2.049(3)	S1−C2	1.780(4)
Pt1−N11	2.039(2)	S1−C3	1.803(4)
S1−Pt1−C1	92.00(9)	C1−Pt1−N21	176.51(11)
S1−Pt1−N11	173.82(6)	N11−Pt1−N21	85.49(8)
S1−Pt1−N21	90.72(6)	P1−S1−C2	111.64(14)
C1−Pt1−N11	91.61(11)	P1−S1−C3	108.31(15)

The complexes Tp′PtMe(CO) (**13**) and Tp′PtMe(CH_2═CH_2) (**14**) are distinctly different from **11** and **12** in that the solid-state IR spectra indicate κ^3 coordination of the Tp′ ligand (ν_{BH} = 2513 cm^{-1} for **13**, ν_{BH} = 2520 cm^{-1} for **14**).[22] The IR spectrum (KBr) of the methyl carbonyl complex **13** displays an absorption for the CO stretch at 2057 cm^{-1}, 40 cm^{-1} lower than in the cationic precursor complex **6**, indicating stronger back-donation into the CO(π*) orbital in the neutral platinum(II) complex.

Comparison with TpPtMe(CO) is appropriate.[9,24] The IR spectrum of TpPtMe(CO) displays an absorption for the CO stretch at 2088 cm^{-1}, 30 cm^{-1} higher than in the Tp′ analogue, which is consistent with stronger donor character for Tp′ versus Tp. The solid-state structure of TpPtMe(CO) is square planar with a bidentate Tp ligand,[25] but the complex is fluxional at room temperature in $CDCl_3$, and at low temperature a trigonal-bipyramidal structure has been inferred from NMR data: two of the three pyrazole rings are magnetically equivalent, and all three show platinum coupling.[9,24b]

In contrast, the solid-state IR data indicates κ^3 coordination of the Tp′ ligand in Tp′PtMe(CO) (**13**), while the solution IR spectrum (hexanes) of **13** shows two absorptions for the B−H stretch (2521, 2478 cm^{-1}) as well as two CO absorptions (2081, 2065 cm^{-1}) (Figure 9). These data clearly indicate that complex **13** exists in solution in both square-planar (ν_{BH} 2478 cm^{-1}, ν_{CO} 2081 cm^{-1}) *and* trigonal bipyramidal (ν_{BH} 2521 cm^{-1}, ν_{CO} 2065 cm^{-1}) geometries. We interpret the NMR data for **13** on the basis of a rapid equilibration between square-planar and trigonal-bipyramidal geometries. It seems reasonable that the ^{11}B NMR chemical shift of −7.38 ppm, which lies between the chemical shifts for four-coordinate square-planar and five-coordinate trigonal-bipyramidal platinum(II), represents the average of both geometrical isomers present in solution. The ^1H NMR spectrum of complex **13** shows mirror symmetry, and both Tp′ methine resonances exhibit platinum coupling (7.4 Hz (1H) and 8.2 Hz (2H)), which is consistent with coordination of all three pyrazole rings to the platinum center. It has previously been observed that platinum coupling to the methine resonance (1H) of the pyrazole ring *trans* to the ligand with a stronger *trans* influence (Me) was smaller than coupling to the other two methine resonances.[26] The two equatorial pyrazole rings in a trigonal-bipyramidal structure are equivalent and the axial pyrazole ligand (*trans* to the methyl group) remains unique. This interpretation is consistent with the presence of a molecular mirror plane on the NMR time scale in the ^1H and ^{13}C NMR spectra even at −80 °C if the barrier for isomer interconversion is low. Although we believe both geometries are present in solution samples, only the infrared time scale is short enough to probe their independent existence.

De Felice and co-workers reported IR data for trigonal-bipyramidal platinum(II) carbonyl complexes of the general formula [PtClR(dmphen)(CO)] (dmphen = 2,9-dimethyl-1,10-phenanthroline) with chloride bound to platinum.[16b] The CO stretching frequencies are observed around 2010 cm^{-1}, 100 cm^{-1} lower than in the square-planar complexes [PtR(dmphen)(CO)][BF_4], while the coupling constants $^1J_{Pt-CO}$ lie in the range of about 2500 Hz, 500 Hz larger than in the square-planar cationic complexes. Similar trends are observed in the present Tp′Pt complexes, cationic **6** and neutral **13**. Upon going from the cationic methyl carbonyl complex **6** to the neutral complex **13**, the CO stretching frequency decreases about 40 cm^{-1}, while the coupling constant $^1J_{Pt-CO}$ increases about 100 Hz.

Trigonal-bipyramidal geometries are common among $TpPt^{II}$ complexes,[24,26,27] as illustrated by the crystal structure of TpPtMe($CF_3C{\equiv}CCF_3$).[28] Several platinum(II) olefin complexes containing chelating nitrogen ligands with σ-donor properties also exhibit trigonal-bipyramidal structures.[24,27,29] The spectroscopic data for Tp′PtMe(CH_2═CH_2) (**14**) indicate a trigonal-bipyramidal geometry: for example, the mirror symmetry observed by ^1H NMR (2:1 pattern for the pyrazole resonances), the solution IR spectrum (B−H stretch at 2536 cm^{-1}), and the ^{11}B NMR chemical shift (−8.72 ppm). The free energy of activation for ethylene rotation was calculated to be 15 kcal/mol at T_c = 388 K in toluene-d_8. Manzer and co-workers reported $^2J_{Pt-H}$ coupling data differentiating $Pt^{II}-CH_3$ and $Pt^{IV}-CH_3$ units for platinum complexes with pyrazole ligands. $^2J_{Pt-H}$ for a platinum(II)-bound methyl group *trans* to a pyrazole substituent lies near 75 Hz, while in platinum(IV) complexes is it considerably smaller, about 64 Hz.[26] $^2J_{Pt-H}$ for the platinum-bound methyl group in ethylene complex **14** is 65.3 Hz, clearly in the platinum(IV) range.

(24) (a) Clark, H. C.; Manzer, L. E. *J. Am. Chem. Soc.* **1973**, *95*, 3812. (b) Clark, H. C.; Manzer, L. E. *Inorg. Chem.* **1974**, *13*, 1996.
(25) Oliver, J. D.; Rush, P. E. *J. Organomet. Chem.* **1976**, *104*, 117.
(26) Clark, H. C.; Manzer, L. E. *Inorg. Chem.* **1974**, *13*, 1291.
(27) For crystal structures of trigonal-bipyramidal platinum(II) ethylene complex see e.g.: (a) Mink, L.; Rettig, M. F.; Wing, R. M. *J. Am. Chem. Soc.* **1991**, *113*, 2065. (b) Bavoso, A.; Funicello, M.; Morelli, G.; Pavone, V. *Acta Crystallogr.* **1984**, *C40*, 2035.
(28) Davies, B. W.; Payne, N. C. *Inorg. Chem.* **1974**, *13*, 1843.
(29) See e.g.: (a) Bartolucci, S.; Carpinelli, P.; De Felice, V.; Giovanniti, B.; De Renzi, A. *Inorg. Chim. Acta* **1992**, *197*, 51. (b) Albano, V. G.; Demartin, F.; De Renzi, A.; Morelli, G.; Saporito, A. *Inorg. Chem.* **1985**, *24*, 2032.

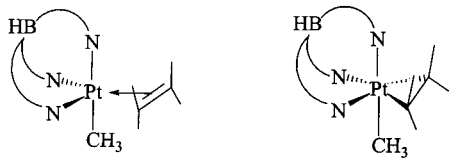

Figure 10. Trigonal-bipyramidal versus octahedral representation of complex **14**.

Certainly both resonance structures shown above for **14** are legitimate (Figure 10), but the platinum(IV) octahedral metallacyclopropane depiction is particularly convenient for correctly predicting properties (e.g. coupling constants, chemical shifts, and olefin orientation).

The ^{1}H NMR spectrum of Tp′PtPh(NCMe) (**15**) indicates a chiral metal center. Two multiplets are observed for the platinum-bound phenyl group at 6.8 ppm. The carbon atoms of the coordinated acetonitrile molecule resonate at 115.1 ppm (N*C*CH$_3$) and 4.2 ppm (NC*C*H$_3$). The solid-state IR spectrum of **15** shows an absorption at 2474 cm^{-1} for the B−H stretch of the Tp′ ligand, indicating κ^2 coordination.

Conclusion

The platinum(IV) complexes Tp′PtMe$_2$H (**1**) and Tp′PtPh$_2$H (**2**) undergo protonation selectively at a pyrazole nitrogen atom, which in turn promotes reductive elimination of methane or benzene, respectively. The resulting three-coordinate platinum(II) intermediates can be trapped with a variety of ligands, and the synthesis and structure of various cationic platinum(II) complexes with the protonated hydridotris(3,5-dimethylpyrazolyl)borate ligand have been reported. Evidence for the intermediacy of a σ-methane complex in the protonation of the dimethyl hydride **1** is provided by the protonation of Tp′PtMe$_2$D (**1-*d***), which leads to deuterium scrambling into the platinum-bound methyl group. A synthetic protocol has been developed which leads to the synthesis of neutral Tp′Pt^{II} complexes via a protonation−trapping−deprotonation sequence. While complexes containing σ-donor ligands display simple square-planar geometries with a free Tp′ arm, complexes containing a π-acid ligand, either CO or ethylene, bind the third pyrazole arm to platinum. In the case of the methyl carbonyl complex **13**, the four-coordinate square-planar and five-coordinate trigonal-bipyramidal structures rapidly interconvert in solution, while the methyl ethylene complex **14** is five-coordinate with a tridentate Tp′ ligand.

Experimental Section

Materials and Methods. Reactions were performed under an atmosphere of dry nitrogen or argon using standard Schlenk and drybox techniques. Argon and nitrogen were purified by passage through columns of BASF R3-11 catalyst and 4 Å molecular sieves. All glassware was oven-dried before use. Methylene chloride, acetonitrile, diethyl ether, and pentanes were purified under an argon atmosphere by passage through a column packed with activated alumina.[30] Tetrahydrofuran was freshly distilled from sodium benzophenone ketyl prior to use. Deuterated methylene chloride was vacuum transferred from calcium hydride and degassed by several freeze−pump−thaw cycles. Deuterated tetrahydrofuran was vacuum-transferred from sodium benzophenone ketyl and degassed.

Tp′Pt(CH$_3$)$_2$H,[4a] Tp′Pt(C$_6$H$_5$)$_2$H,[4a] and [H(OEt$_2$)$_2$][BAr′$_4$][11] were synthesized according to published procedures. Carbon monoxide was obtained from Matheson Gas Products Inc. and ^{13}C-labeled carbon monoxide from Cambridge Isotope Laboratories Inc. All other reagents were used as obtained from commercial sources.

^{1}H NMR, ^{13}C NMR, and ^{31}P NMR spectra were recorded on a Bruker Avance 400 spectrometer and ^{2}H NMR and ^{11}B NMR spectra on a Bruker Avance 500 spectrometer. ^{1}H NMR and ^{13}C NMR chemical shifts were referenced to residual ^{1}H and ^{13}C signals of the deuterated solvents. ^{31}P NMR shifts were referenced to 85% H$_3$PO$_4$, while ^{11}B NMR shifts were referenced to BF$_3$·Et$_2$O. Infrared spectra were recorded on an ASI ReactIR 1000. Chemical analyses were performed by Atlantic Microlabs of Norcross, GA.

Tp′Pt(CH$_3$)$_2$D (1-*d*). Tp′Pt(CH$_3$)$_2$H (90 mg, 0.17 mmol) was dissolved in 10 mL of THF, and the solution was cooled to −78 °C. While the solution was stirred, ^{n}BuLi (2.5 M in hexane, 0.1 mL) was added. The solution was stirred for about 15 min and then slowly warmed to room temperature and stirred for another 2 h. The reaction mixture was quenched with 0.3 mL of D$_2$O. The solvent was removed in vacuo, and the residue was washed with acetonitrile. A 50 mg amount of **1-*d***, including about 10% Tp′Pt(CH$_3$)$_2$H, was collected as a white solid. Yield: 56%. ^{1}H NMR (CD$_2$Cl$_2$, δ): 5.84 (s, 1H, Tp′C*H*), 5.82 (s, 2H, Tp′C*H*), 2.40, 2.35, 2.31, 2.22 (s, 3H, 6H, 3H, 6H, Tp′C*H*$_3$), 1.20 (s, 6H, $^2J_{Pt-H}$ = 67 Hz, Pt(C*H*$_3$)$_2$), −20.90 (s, 0.1 H, $^1J_{Pt-H}$ = 1361 Hz, Pt-*H*).

Representative [BAr′$_4$]$^-$ NMR Data. ^{1}H and ^{13}C NMR data for the [BAr′$_4$]$^-$ counterion are reported separately for simplicity. ^{1}H NMR (CD$_2$Cl$_2$, δ): 7.77 (br, 8H, *o*-Ar′), 7.60 (br, 4H, *p*-Ar′). ^{13}C NMR (CD$_2$Cl$_2$, δ): 162.2 (1:1:1:1 pattern, $^1J_{B-C}$ = 50 Hz, C$_{ipso}$), 135.3 (C$_{ortho}$), 129.4 (qq, $^2J_{C-F}$ = 30 Hz, $^4J_{C-F}$ = 5 Hz, C$_{meta}$), 125.1 (q, $^1J_{C-F}$ = 270 Hz, *C*F$_3$), 117.9 (C$_{para}$).

Protonation of Tp′Pt(CH$_3$)$_2$H (1), Tp′Pt(CH$_3$)$_2$D (1-*d*), and Tp′Pt(C$_6$H$_5$)$_2$H (2). The samples were prepared under an argon atmosphere in a drybox. Equimolar amounts of a [Tp′Pt^{IV}] complex and [H(OEt$_2$)$_2$][BAr′$_4$] were weighed into an NMR tube, which was then sealed with a septum and secured with Teflon tape. The NMR tube was cooled to −78 °C outside the drybox, and about 0.5 mL of CD$_2$Cl$_2$ was slowly added through the septum.

1 + Acid. ^{1}H NMR (CD$_2$Cl$_2$, 193 K, δ): 11.66 (s, 1H, pz*N*H), 6.09, 5.97, 5.89 (s, 1H each, HTp′C*H*), 2.29, 2.26, 2.25, 2.20, 2.14, 1.59 (s, 3H each, HTp′C*H*$_3$), 0.39 (s, 3H, PtC*H*$_3$), 0.14 (s, C*H*$_4$). ^{13}C NMR (CD$_2$Cl$_2$, 193 K, δ): 151.5, 150.6, 148.0, 147.6, 147.2, 143.5 (HTp′*C*CH$_3$), 108.8, 107.4, 106.8 (HTp′*C*H), 14.4, 13.1, 13.0, 12.6, 11.1, 10.7 (HTp′*C*H$_3$), −4.1 (*C*H$_4$), −22.4 (Pt−*C*H$_3$).

1-*d* + Acid. ^{1}H NMR (CD$_2$Cl$_2$, 193K, δ): 11.77 (s, 1H, pz*N*H), 6.10, 5.97, 5.90 (s, 1H each, HTp′C*H*), 2.30, 2.26, 2.25, 2.20, 2.15, 1.61 (s, 3H each, HTp′C*H*$_3$), 0.40, 0.38 (s, ca. 2H, PtC*H*$_3$), 0.14 (s, C*H*$_4$), 0.13 (1:1:1, C*H*$_3$D).

2 + Acid. ^{1}H NMR (CD$_2$Cl$_2$, 193 K, δ): 11.82 (s, 1H, pz*N*H), 7.33 (s, 6H, C$_6$H$_6$), 6.84 (br, 5H, Pt−C$_6$*H*$_5$), 6.22, 5.98, 5.84 (s, 1H each, HTp′C*H*), 2.34, 2.33, 2.30, 2.23, 1.76, 1.47 (s, 3H each, HTp′C*H*$_3$). ^{13}C NMR (CD$_2$Cl$_2$, 193 K, δ): 153.0, 151.4, 148.5, 147.8, 144.1 (HTp′*C*CH$_3$), 126.7, 123.9 (Pt-*C*$_6$H$_5$), 109.4, 107.9, 107.4 (HTp′*C*H), 14.7, 13.2, 13.1, 12.6, 11.4, 10.9 (HTp′*C*H$_3$).

Representative Synthesis of [κ^2-((Hpz*)BHpz*$_2$)Pt(Me,Ph)(L)][BAr′$_4$] Complexes (3−10). In a typical experiment, 0.1 g of Tp′Pt(CH$_3$)$_2$H in CH$_2$Cl$_2$ (10 mL) was cooled to −78 °C. In a separate Schlenk flask, a CH$_2$Cl$_2$ solution (10

(30) Pangborn, A. B.; Giardello, M. A.; Grubbs, R. H.; Rosen, R. K.; Timmers, F. J. *Organometallics* **1996**, *15*, 1518.

mL) of $[H(OEt_2)_2][BAr'_4]$ (1 equiv) was cooled to −78 °C. The $[H(OEt_2)_2][BAr'_4]$ solution was transferred via cannula to the flask containing the $Tp'Pt(CH_3)_2H$ solution. The reaction mixture was stirred for ca. 15 min, the trapping ligand was added, and the reaction mixture was warmed to ambient temperature. The solvent was removed in vacuo, and the residue was triturated with pentane before it was recrystallized from an appropriate solvent mixture.

[κ²-((Hpz*)BHpz*₂)Pt(CH₃)(NCCH₃)][BAr′₄] (3). $Tp'Pt(CH_3)_2H$ (70 mg, 0.13 mmol), $[H(OEt_2)_2][BAr'_4]$ (135 mg, 0.13 mmol), and 2 mL of CH_3CN were combined as described above. Colorless crystals were obtained from CH_2Cl_2/pentanes. Yield: 110 mg (58%). ^{1}H NMR (CD_2Cl_2, δ): 12.22 (br, 1H, pz*N*H*), 6.17, 6.00, 5.97 (s, 1H each, HTp′C*H*), 2.36, 2.35, 2.34, 2.29, 2.27, 2.20 (s, 3H, 3H, 6H, 3H, 3H, 3H, HTp′C*H*$_3$ and Pt−NCC*H*$_3$), 0.66 (s, 3H, $^2J_{Pt-H}$ = 76 Hz, Pt−C*H*$_3$). ^{1}H NMR (CD_2Cl_2, 193 K, δ): 12.59 (s, 1H, pz*N*H*), 6.08, 5.95, 5.92 (s, 1H each, HTp′C*H*), 2.35, 2.27, 2.25, 2.21, 2.10 (s, 3H, 3H, 6H, 6H, 3H, HTp′C*H*$_3$ and Pt−NCC*H*$_3$), 0.55 (s, 3H, Pt−C*H*$_3$). ^{13}C NMR (CD_2Cl_2, 193 K, δ): 151.5, 149.9, 148.1, 147.4, 146.5, 142.5 (HTp′*C*CH$_3$), 116.7 (Pt−N*C*CH$_3$), 107.7, 107.3, 106.5 (HTp′*C*H), 14.3, 13.36, 13.32, 12.8, 11.9, 10.8 (HTp′*C*H$_3$), 4.1 (Pt−NC*C*H$_3$), −21.5 ($^1J_{Pt-C}$ = 641 HZ, Pt−*C*H$_3$). Anal. Calcd for $C_{50}H_{41}N_7B_2F_{24}Pt$: C, 42.51; H, 2.93; N, 6.94. Found: C, 42.56; H, 2.92; N, 6.86.

[κ²-((Hpz*)BHpz*₂)Pt(CH₃)(CN^{t}Bu)][BAr′₄] (4). $Tp'Pt(CH_3)_2H$ (100 mg, 0.19 mmol), $[H(OEt_2)_2][BAr'_4]$ (195 mg, 0.19 mmol), and 0.022 mL of ^{t}BuNC (16 mg, 0.20 mmol) were combined as described above. The yellow solution was filtered through a plug of Celite. Light yellow crystals were obtained from diethyl ether/pentanes. Diethyl ether free **4** was obtained after a second recrystallization from CH_2Cl_2/pentanes. Yield: 123 mg (44%). ^{1}H NMR (CD_2Cl_2, δ): 10.76 (br, 1H, pz*N*H*), 6.17, 6.04, 6.00 (s, 1H each, HTp′C*H*), 2.37, 2.35, 2.32, 2.31, 2.27, 1.99 (s, 3H each, HTp′C*H*$_3$), 1.46 (s, 9H, Pt−NC^t*Bu*), 0.60 (s, 3H, $^2J_{Pt-H}$ = 76 Hz, Pt−C*H*$_3$). ^{13}C NMR (CD_2Cl_2, δ): 153.0, 152.0, 149.8, 148.6, 148.0, 143.8 (HTp′*C*CH$_3$), 109.4, 108.8, 107.9 (HTp′*C*H), 59.2 (*C*(CH$_3$)$_3$), 30.2 (C(*C*H$_3$)$_3$), 14.8, 14.6, 13.4, 13.2, 11.9, 11.2 (HTp′*C*H$_3$), −23.4 (Pt-*C*H$_3$, $^1J_{Pt-C}$ = 589 Hz). Anal. Calcd for $C_{53}H_{47}N_7B_2F_{24}Pt$: C, 43.76; H, 3.26; N, 6.74. Found: C, 43.98; H, 3.39; N, 6.51.

[κ²-((Hpz*)BHpz*₂)Pt(CH₃)(NC₅H₅)][BAr′₄] (5). $Tp'Pt(CH_3)_2H$ (120 mg, 0.23 mmol), $[H(OEt_2)_2][BAr'_4]$ (240 mg, 0.24 mmol), CH_2Cl_2, and 0.03 mL of C_5H_5N (29 mg, 0.37 mmol) were combined as described above. Colorless crystals were obtained from diethyl ether/pentanes. Diethyl ether free **5** was obtained after a second recrystallization from CH_2Cl_2/pentanes. Yield: 228 mg (69%). ^{1}H NMR (CD_2Cl_2, δ): 13.81 (br, 1H, pz*N*H*), 8.35 (d of d, 2H, $^3J_{H-H}$ = 6.4 Hz, $^4J_{H-H}$ = 1.5 Hz, $^3J_{Pt-H}$ = 44 Hz, C$_{ortho}$, Pt−NC$_5$H$_5$), 7.85 (t of t, 1H, $^3J_{H-H}$ = 7.6 Hz, $^4J_{H-H}$ = 1.5 Hz, C$_{para}$, Pt−NC$_5$H$_5$), 7.32 (d of d, 2H, $^3J_{H-H}$ = 7.6 Hz, $^3J_{H-H}$ = 6.4 Hz, C$_{meta}$, Pt−NC$_5$H$_5$), 6.19, 6.03, 5.88 (s, 1H each, HTp′C*H*), 2.44, 2.41, 2.38, 2.35, 2.25, 1.47 (s, 3H each, HTp′C*H*$_3$), 0.81 (s, 3H, $^2J_{Pt-H}$ = 76 Hz, Pt−C*H*$_3$). ^{13}C NMR (CD_2Cl_2, δ, 303 K): 153.3, 150.7, 149.8, 148.9, 147.5, 143.8 (HTp′*C*CH$_3$), 152.3 (C$_{meta}$, Pt−NC$_5$H$_5$), 138.8 (C$_{para}$, Pt−NC$_5$H$_5$), 127.2 (C$_{ortho}$, $^2J_{Pt-C}$ = 46 Hz), 108.75, 108.7, 108.2 (HTp′*C*H), 14.8, 13.7, 13.4, 12.7, 12.6, 11.1 (HTp′*C*H$_3$), −16.1 (Pt-*C*H$_3$, $^1J_{Pt-C}$ = 725 Hz). Anal. Calcd for $C_{53}H_{43}N_7B_2F_{24}Pt$: C, 43.88; H, 2.99; N, 6.76. Found: C, 44.43; H, 2.93; N, 6.63.

[κ²-((Hpz*)BHpz*₂)Pt(CH₃)(CO)][BAr′₄] (6). $Tp'Pt(CH_3)_2H$ (600 mg, 1.15 mmol) and $[H(OEt_2)_2][BAr'_4]$ (1.195 g, 1.18 mmol) were combined as described above. Carbon monoxide gas was purged through the solution while it was warmed to room temperature (ca. 20 min). Colorless crystals were obtained from THF/pentanes. Yield: 0.988 g (59%). IR (KBr): ν_{BH} 2518 cm^{-1}, ν_{CO} 2099 cm^{-1}. ^{1}H NMR (CD_2Cl_2, 293 K, δ): 11.29 (br, 1H, pz*N*H*), 6.19, 6.07, 6.06 (s, 1H each, HTp′C*H*), 2.40, 2.38, 2.35, 2.29, 2.28 1.72 (s, 3H each, HTp′C*H*$_3$), 0.82 (s, 3H, $^2J_{Pt-H}$ = 73 Hz, Pt−C*H*$_3$). ^{13}C NMR (CD_2Cl_2, 293 K, δ): 164.0 ($^1J_{Pt-C}$ = 1877 Hz, Pt−*C*O), 153.6, 152.5, 150.1, 149.9, 149.1, 145.4 (HTp′*C*CH$_3$), 110.3, 109.3, 108.3 (HTp′*C*H), 14.8, 14.6, 13.3, 13.0, 11.5, 10.9 (HTp′*C*H$_3$), −19.9 ($^1J_{Pt-C}$ = 523 Hz, Pt−*C*H$_3$). Anal. Calcd for $C_{49}H_{38}N_6B_2F_{24}OPt\cdot C_4H_8O$: C, 43.26; H, 3.15; N, 5.71. Found: C, 43.48; H, 3.13; N, 5.59.

[κ²-((Hpz*)BHpz*₂)Pt(CH₃)(CH₂═CH₂)][BAr′₄] (7). $Tp'Pt(CH_3)_2H$ (150 mg, 0.29 mmol) and $[H(OEt_2)_2][BAr'_4]$ (290 mg, 0.29 mmol) were combined as described above. Ethylene gas was purged through the solution while it was warming to room temperature (ca. 20 min). Colorless crystals were obtained from CH_2Cl_2/pentanes. Yield: 226 mg (56%). ^{1}H NMR (CD_2Cl_2, 293 K, δ): 9.76 (br, 1H, pz*N*H*), 6.27, 6.11, 5.94 (s, 1H each, HTp′C*H*), 3.88, 3.69 (m, 2H each, broad Pt satellites, J_{Pt-H} = 69 Hz, Pt-bound CH$_2$═CH$_2$), 2.39, 2.36, 2.35, 2.21, 1.87 (s, 3H, 3H, 6H, 3H, 3H, HTp′C*H*$_3$), 0.24 (s, 3H, $^2J_{Pt-H}$ = 72 Hz, Pt−C*H*$_3$). ^{13}C NMR (CD_2Cl_2, 293 K, δ): 152.9, 152.3, 150.1, 149.2, 144.5 (HTp′*C*CH$_3$), 110.3, 109.2 (1C, 2C, HTp′*C*H), 69.5 (s, $^1J_{Pt-C}$ = 200 Hz, Pt-bound ethylene), 14.5, 14.1, 13.30, 13.27, 11.8, 11.2 (HTp′*C*H$_3$), −13.5 (s, $^1J_{Pt-C}$ = 632 Hz, Pt−*C*H$_3$). Anal. Calcd for $C_{50}H_{42}N_6B_2F_{24}Pt$: C, 42.91; H, 3.02; N, 6.00. Found: C, 42.66; H, 3.07; N, 6.05.

[κ²-((Hpz*)BHpz*₂)Pt(CH₃)(PMe₂Ph)][BAr′₄] (8). In an NMR tube, $Tp'Pt(CH_3)_2H$ (9 mg, 0.02 mmol) and $[H(OEt_2)_2][BAr'_4]$ (19 mg, 0.02 mmol) were dissolved in 0.6 mL of CD_2Cl_2 at −78 °C. A 2.4 μL portion of PMe_2Ph was added through the septum. Next, the solution was layered with pentane and kept in a freezer for 4 weeks. Colorless crystals were obtained and dried in vacuo. Yield: 10 mg (38%). ^{1}H NMR (CD_2Cl_2, δ): 10.42 (br, 1H, pz*N*H*), 7.58−7.39 (m, 5H, Pt−PMe$_2$C$_6$*H*$_5$), 6.30, 6.07, 5.84 (s, 1H each, HTp′C*H*), 2.39, 2.37, 2.33, 2.23, 1.85 (s, 3H, 3H, 6H, 3H, 3H, HTp′C*H*$_3$), 1.48, 1.37 (d, 3H each, $^2J_{P-H}$ = 10.3 Hz, $^3J_{Pt-H}$ = 45 Hz, Pt−P(C*H*$_3$)$_2$Ph), 0.45 (d, 3H, $^3J_{P-H}$ = 4.9 Hz, $^2J_{Pt-H}$ = 72 Hz, Pt−C*H*$_3$). ^{13}C NMR (CD_2Cl_2, δ): 152.8, 150.9, 149.4, 149.0, 148.3, 143.5 (HTp′*C*CH$_3$), 131.9, 131.74, 131.67, 129.2 (PMe$_2$*C*$_6$H$_5$), 109.6, 108.8, 107.9 (HTp′*C*H), 15.3, 14.6, 13.5, 13.3, 12.4, 11.4 (HTp′*C*H$_3$), 14.2, 13.6 (d, $^1J_{P-C}$ = 42 Hz, P(*C*H$_3$)$_2$Ph), −19.3 (d, $^2J_{P-C}$ = 9 Hz, $^1J_{Pt-C}$ = 642 Hz, Pt−*C*H$_3$). ^{31}P NMR (CD_2Cl_2, δ): −17.9 ppm (s, $^1J_{Pt-P}$ = 4114 Hz). Anal. Calcd for $C_{56}H_{49}N_6B_2F_{24}PPt\cdot CD_2Cl_2$: C, 42.88; H, 3.35; N, 5.26. Found: C, 43.28; H, 3.58 (H + D as H); N, 5.18.

[κ¹-((Hpz*)BHpz*₂)Pt(CH₃)(PMe₂Ph)₂][BAr′₄] (9). $Tp'Pt(CH_3)_2H$ (120 mg, 0.23 mmol), $[H(OEt_2)_2][BAr'_4]$ (240 mg, 0.24 mmol), and 0.06 mL of PMe_2Ph (58 mg, 0.42 mmol) were combined as described above. White crystals were obtained from CH_2Cl_2/pentanes. Yield: 212 mg (56%). ^{1}H NMR (CD_2Cl_2, 303 K, δ): 11.74 (br, 1H, pz*N*H*), 7.71, 7.47 (m, 10H, Pt−PMe$_2$C$_6$*H*$_5$), 6.03, 5.87 (s, 2H, 1H, HTp′C*H*), 2.32, 2.29, 2.24, 1.75 (s, 6H, 6H, 3H, 3H, HTp′C*H*$_3$), 1.52, 1.12 (t, 6H each, $^2J_{P-H}$ = 3.4 Hz, $^3J_{Pt-H}$ = 30 Hz, Pt−P(C*H*$_3$)$_2$Ph), 0.32 (t, 3H, $^3J_{P-H}$ = 7.3 Hz, $^2J_{Pt-H}$ = 72 Hz, Pt−C*H*$_3$). ^{13}C NMR (CD_2Cl_2, 303 K, δ): 150.5, 148.6, 148.4, 148.3 (HTp′*C*CH$_3$), 133.6, 132.1, 131.2, 129.2 (PMe$_2$*C*$_6$H$_5$), 109.5, 108.4 (HTp′*C*H), 15.7, 13.2, 12.6, 12.0 (HTp′*C*H$_3$), 12.7, 11.6 (t, $^1J_{P-C}$ = 17 Hz, P(*C*H$_3$)$_2$Ph), −20.1 (t, $^2J_{P-C}$ = 7 Hz, $^1J_{Pt-C}$ = 613 Hz, Pt−*C*H$_3$). ^{31}P NMR (CD_2Cl_2, δ): −0.87 ppm (s, $^1J_{Pt-P}$ = 2942 Hz). Anal. Calcd for $C_{64}H_{60}N_6B_2F_{24}P_2Pt$: C, 46.65; H, 3.67; N, 5.10. Found: C, 46.83; H, 3.67; N, 5.07.

[κ²-((Hpz*)BHpz*₂)Pt(C₆H₅)(NCCH₃)][BAr′₄] (10). $Tp'Pt(C_6H_5)_2H$ (70 mg, 0.11 mmol), $[H(OEt_2)_2][BAr'_4]$ (110 mg, 0.11 mmol), and 3 mL of CH_3CN were combined as described above. An off-white solid was obtained from diethyl ether/pentanes. Yield: 82 mg (52%). ^{1}H NMR (CD_2Cl_2, δ): 12.38 (br, 1H, pz*N*H*), 6.95 (m, 3H, H$_{meta}$ and H$_{para}$, Pt−C$_6$H$_5$), 6.82 (m, 2H, $^3J_{Pt-H}$ = 44 Hz, H$_{ortho}$, Pt−C$_6$H$_5$), 6.24 (d, 1H, $^4J_{H-H}$ = 1.6 Hz, Hpz*C*H*), 6.05, 5.90 (s, 1H each, pz*C*H*), 2.403, 2.396, 2.39, 2.37, 2.31, 2.29, 1.53 (s, 3H each, HTp′C*H*$_3$ and Pt−NCC*H*$_3$). ^{1}H NMR (CD_2Cl_2, 193 K, δ): 12.26 (s, 1H, pz*N*H*), 6.85 (br, 3H, H$_{meta}$ and H$_{para}$, Pt−C$_6$H$_5$), 6.72 (br, 2H, H$_{ortho}$, Pt−C$_6$H$_5$), 6.16, 5.98, 5.85 (s, 1H each, HTp′C*H*), 2.37, 2.332, 2.325, 2.29, 2.26, 1.95, 1.41 (s, 3H each, HTp′C*H*$_3$ and Pt−NCC*H*$_3$). ^{13}C NMR (CD_2Cl_2, δ): 153.9, 152.3, 149.9, 148.6, 146.5, 144.2

Table 9. Crystallographic Data Collection Parameters

	3	6	7	8	9	12
formula	$C_{50}H_{41}B_2F_{24}N_7Pt$	$C_{53}H_{46}B_2F_{24}N_6O_2Pt$	$C_{50}H_{42}B_2F_{24}N_6Pt$	$C_{57}H_{50}B_2Cl_2F_{24}N_6PPt$	$C_{64}H_{60}B_2F_{24}N_6P_2Pt$	$C_{18}H_{31}BN_6SPt$
mol wt	1412.58	1471.64	1399.58	1593.60	1647.82	569.44
cryst syst	triclinic	triclinic	triclinic	triclinic	monoclinic	monoclinic
space group	$P\bar{1}$	$P\bar{1}$	$P\bar{1}$	$P\bar{1}$	$P2_1/c$	$P2_1/c$
a, Å	12.6683(6)	12.8583(6)	13.0249(5)	14.3058(7)	13.0098(7)	16.2303(4)
b, Å	13.2799(6)	12.9407(6)	13.1185(5)	14.8057(7)	27.2034(14)	8.50990(20)
c, Å	18.9746(9)	18.6034(8)	18.1205(6)	16.2241(7)	19.7507(10)	17.1741(4)
α, deg	99.488(1)	76.164(1)	75.995(1)	89.352(1)		
β, deg	91.418(1)	86.584(1)	89.703(1)	69.624(1)	93.723(1)	111.752(1)
γ, deg	117.656(1)	75.713(1)	68.347(1)	87.030(1)		
V, Å^3	2769.99(22)	2912.74(23)	2780.00(18)	3217.0(3)	6975.2(6)	2203.16(9)
Z	2	2	2	2	4	4
calcd density, Mg/m^3	1.694	1.678	1.672	1.645	1.569	1.717
F(000)	1386.76	1450.80	1374.74	1573.59	3278.49	1115.92
cryst dimens, mm	0.25 × 0.30 × 0.30	0.25 × 0.25 × 0.20	0.40 × 0.25 × 0.15	0.20 × 0.20 × 0.15	0.40 × 0.30 × 0.15	0.35 × 0.20 × 0.20
temp, °C	−100					
radiation (*λ*, Å)	Mo Kα (0.710 73)					
2*θ* range, deg	3−50	3−50	3−60	3−56	3−56	5−70
μ, mm^{-1}	2.65	2.52	2.64	2.39	2.16	6.45
scan mode	*ω*					
total no. of rflns	14 091	22 936	45 894	51 044	17 625	88 726
total no. of unique rflns	9227	13 679	16 313	15 568	16 932	9735
no. of obsd data ($I > 2.5\sigma(I)$)	7856	9239	13 013	13 219	14 255	8897
R_F, %	0.031	0.062	0.035	0.040	0.048	0.028
R_w, %	0.038	0.051	0.040	0.044	0.044	0.041
GOF	1.21	1.2065	1.9189	1.5135	3.1767	1.9584

(HTp′*C*CH$_3$), 136.2, 127.6, 124.7 (Pt−*C*$_6$H$_5$), 117.5 (Pt−N*C*CH$_3$), 109.4, 108.9, 108.4 (HTp′*C*H), 15.2, 14.1, 13.8, 13.2, 12.5, 11.4 (HTp′*C*H$_3$), 4.2 (Pt−NC*C*H$_3$). Anal. Calcd for $C_{55}H_{43}N_7B_2F_{24}Pt\cdot OC_4H_{10}$: C, 45.76; H, 3.45; N, 6.33. Found: C, 45.49; H, 3.47; N, 5.90.

Synthesis of [κ^2-((Hpz*)BHpz*$_2$)Pt(Me)(NCMe)][BF$_4$] (3a). A 0.200 g amount of Tp′Pt(CH$_3$)$_2$H (0.38 mmol) in CH_2Cl_2 (15 mL) was cooled to −78 °C. A 0.06 mL portion of $HBF_4\cdot Et_2O$ (54 wt %) was added dropwise. The cold bath was removed after 15 min, and 2 mL of CH_3CN was added 3 min later. The reaction mixture was warmed to ambient temperature. The solvent was removed in vacuo, and the residue was triturated with pentanes. Recrystallization from CH_2Cl_2/pentanes yielded 123 mg (51% yield) of colorless crystals as well as some noncrystalline material. ^{1}H NMR (CD_2Cl_2, *δ*): 11.65 (br, 1H, pz*N*H), 6.14, 6.01, 5.93 (s, 1H each, HTp′C*H*), 2.41, 2.38, 2.37, 2.35, 2.28, 2.25, 1.84 (s, 3H each, HTp′C*H*$_3$ and Pt−NCC*H*$_3$), 0.40 (s, 3H, $^2J_{Pt-H}$ = 76 Hz, Pt−C*H*$_3$). ^{13}C NMR (CD_2Cl_2, *δ*): 152.03, 152.0, 148.0, 147.4 (2C), 144.7 (HTp′*C*CH$_3$), 117.1 (Pt−N*C*CH$_3$), 108.9, 107.9, 107.7 (HTp′*C*H), 13.7, 13.6, 13.5, 12.8, 11.7, 10.9 (HTp′*C*H$_3$), 3.7 (Pt−NC*C*H$_3$), −23.7 ($^1J_{Pt-C}$ = 661 Hz, Pt−*C*H$_3$). Anal. Calcd for $C_{18}H_{29}N_7B_2F_4Pt$: C, 33.95; H, 4.59; N, 15.41. Found: C, 33.75; H, 4.64; N, 15.20.

Representative Synthesis of Tp′Pt(Me)(L) Complexes (11−15). A 0.300 g amount of Tp′Pt(CH$_3$)$_2$H (0.57 mmol) in CH_2Cl_2 (20 mL) was cooled to −78 °C. A 0.1 mL portion of $HBF_4\cdot Et_2O$ (54 wt %) was added dropwise. The cold bath was removed, and the trapping ligand was added after 3 min. The reaction mixture was warmed to ambient temperature. The solvent was removed by rotary evaporation, and the residue was triturated with pentanes. After 18 mg of NaH (0.75 mmol) was added to the flask, it was cooled to −78 °C. A 20 mL amount of THF was slowly added, the cold bath was removed, and the solution was stirred for 1 h. The solvent was then removed by rotary evaporation. After chromatography on alumina (CH_2Cl_2 as eluent), a white solid was obtained, which was washed with cold pentanes and dried in vacuo.

Tp′Pt(CH$_3$)(NCCH$_3$) (11). A 0.300 g amount of Tp′Pt(CH$_3$)$_2$H (0.57 mmol), 0.1 mL of $HBF_4\cdot Et_2O$, 3 mL of CH_3CN, and 18 mg of NaH (0.75 mmol) were combined as described above. Yield: 166 mg (53%). IR (KBr): ν_{BH} 2459 cm^{-1}. IR (CH_2Cl_2): ν_{BH} 2478 cm^{-1}. ^{1}H NMR (CD_2Cl_2, *δ*): 5.864, 5.859, 5.71 (s, 1H each, Tp′C*H*), 2.37, 2.35, 2.25, 2.24, 2.16, 1.62 (s, 3H, 3H, 6H, 3H, 3H, 3H, Tp′C*H*$_3$ and Pt−NCC*H*$_3$), 0.38 (s, 3H, $^2J_{Pt-H}$ = 77 Hz, Pt−C*H*$_3$). ^{13}C NMR (CD_2Cl_2, *δ*): 149.8, 148.1, 147.1, 146.3, 145.8, 142.8 (Tp′*C*CH$_3$), 114.9 (Pt−N*C*CH$_3$), 106.8, 105.8, 105.3 (Tp′*C*H), 14.7, 13.9, 13.8, 13.7, 13.1, 11.4 (Tp′*C*H$_3$), 4.2 (Pt−NC*C*H$_3$), −23.7 ($^1J_{Pt-C}$ = 668 Hz, Pt-*C*H$_3$). ^{11}B NMR (THF-d_8, *δ*): −6.12. Anal. Calcd for $C_{18}H_{28}N_7BPt$: C, 39.42; H, 5.15; N, 17.88. Found: C, 39.47; H, 5.25; N, 17.77.

Tp′Pt(CH$_3$)(SMe$_2$) (12). A 0.200 g amount of Tp′Pt(CH$_3$)$_2$H (0.38 mmol), 0.07 mL of $HBF_4\cdot Et_2O$, 0.1 mL of SMe_2, and 16 mg of NaH (0.67 mmol) were combined as described above. Yield: 70 mg (33%). IR (KBr): ν_{BH} 2455 cm^{-1}. IR (CH_2Cl_2): ν_{BH} 2474 cm^{-1}. ^{1}H NMR (CD_2Cl_2, 243 K, *δ*): 5.90, 5.84, 5.70 (s, 1H each, Tp′C*H*), 2.32, 2.31, 2.22, 2.21, 2.09, 1.52 (s, 3H each, Tp′C*H*$_3$), 2.09 (s, 3H, $^3J_{Pt-H}$ = 57 Hz, Pt−S*Me*$_2$), 1.93 (s, 3H, $^3J_{Pt-H}$ = 51 Hz, Pt−S*Me*$_2$), 0.23 (s, 3H, $^2J_{Pt-H}$ = 75 Hz, Pt−C*H*$_3$). ^{13}C NMR (CD_2Cl_2, 243 K, *δ*): 148.5, 147.3, 146.7, 145.9, 145.3, 142.9 (Tp′*C*CH$_3$), 106.4, 105.41, 105.37 (Tp′*C*H), 21.8, 19.6 (Pt−S*Me*$_2$), 14.2, 13.63, 13.60, 13.5, 13.1, 11.1 (Tp′*C*H$_3$), −20.2 ($^1J_{Pt-C}$ = 708 Hz, Pt−*C*H$_3$). ^{11}B NMR (THF-d_8, *δ*): −6.01. Anal. Calcd for $C_{18}H_{31}N_6BSPt$: C, 37.96; H, 5.49; N, 14.75. Found: C, 38.23; H, 5.60; N, 14.72.

Tp′Pt(CH$_3$)(CO) (13). A 0.300 g amount of Tp′Pt(CH$_3$)$_2$H (0.57 mmol) was combined with 0.1 mL of $HBF_4\cdot Et_2O$. Carbon monoxide gas was purged through the solution while it was warmed to room temperature (ca. 20 min). The reaction was continued by addition of 18 mg of NaH (0.75 mmol). Yield: 167 mg (54%). IR (KBr): ν_{BH} 2513 cm^{-1}, ν_{CO} 2057 cm^{-1}. IR (hexanes): ν_{BH} 2521, 2472 cm^{-1}, ν_{CO} 2081, 2065 cm^{-1};. ^{1}H NMR (CD_2Cl_2, *δ*): 5.92 (s, 1H, $^4J_{Pt-H}$ = 7.4 Hz, Tp′C*H*), 5.84 (s, 2H, $^4J_{Pt-H}$ = 8.2 Hz, Tp′C*H*), 2.37, 2.25, 2.18 (s, 3H, 9H, 6H, Tp′C*H*$_3$), 0.87 (s, 3H, $^2J_{Pt-H}$ = 72.2 Hz, Pt−C*H*$_3$). ^{13}C NMR (CD_2Cl_2, *δ*): 165.1 ($^1J_{Pt-C}$ = 1968 Hz, Pt−*C*O), 149.2 (1C, J_{Pt-C} = 28.1 Hz, Tp′*C*CH$_3$), 149.0 (2C, J_{Pt-C} = 35.8 Hz, Tp′*C*CH$_3$), 146.2 (1C, J_{Pt-C} = 12.6 Hz, Tp′*C*CH$_3$), 144.9 (2C, J_{Pt-C} = 14.5 Hz, Tp′*C*CH$_3$), 106.34 (2C, $^3J_{Pt-C}$ = 17.4 Hz, Tp′*C*H), 106.28 (1C, $^3J_{Pt-C}$ = 13.6 Hz, Tp′*C*H), 15.0 (1C, J_{Pt-C} = 26.2 Hz, Tp′*C*H$_3$), 14.1 (2C, J_{Pt-C} = 10.7 Hz, Tp′*C*H$_3$), 13.2, 12.6 (1C, 2C, Tp′*C*H$_3$), −21.5 ($^1J_{Pt-C}$ = 537 Hz, Pt−*C*H$_3$). ^{11}B NMR (THF-

d_8, δ): −7.38. Anal. Calcd for $C_{17}H_{25}N_6OBPt$: C, 38.14; H, 4.71; N, 15.69. Found: C, 38.35; H, 4.88; N, 15.63.

Tp′Pt(CH$_3$)(CH$_2$=CH$_2$) (14). A 0.300 g amount of Tp′Pt(CH$_3$)$_2$H (0.57 mmol) was combined with 0.1 mL of HBF_4·Et_2O. Ethylene gas was purged through the solution while it was warmed to room temperature (ca. 20 min); then 18 mg of NaH (0.75 mmol) was added. Yield: 140 mg (46%). IR (KBr): ν_{BH} 2520 cm^{-1}. IR (CH_2Cl_2): ν_{BH} 2536 cm^{-1}. ^{1}H NMR (CD_2Cl_2, 253 K, δ): 5.88, 5.60 (s, 2H, 1H, Tp′C*H*), 3.03 (d, 2H, $^3J_{H-H}$ = 7.0 Hz, $^2J_{Pt-H}$ = 83.3 Hz, Pt−CH$_2$=C*H*$_2$), 2.37, 2.26, 2.07 (s, 6H, 9H, 3H, Tp′C*H*$_3$), 1.88 (d, 2H, $^3J_{H-H}$ = 7.0 Hz, $^2J_{Pt-H}$ = 83.3 Hz, Pt−CH$_2$=C*H*$_2$), 0.42 (s, 3H, $^2J_{Pt-H}$ = 65.3 Hz, Pt−C*H*$_3$). ^{13}C NMR (CD_2Cl_2, 253 K, δ): 150.5 (1C, $^2J_{Pt-C}$ = 17.4 Hz, Tp′*C*CH$_3$), 149.4 (2C, $^2J_{Pt-C}$ = 42.6 Hz, Tp′*C*CH$_3$), 144.2, 144.0 (1C, 2C, Tp′*C*CH$_3$), 107.6 (1C, Tp′*C*H), 105.9 (2C, $^3J_{Pt-C}$ = 15.5 Hz, Tp′*C*H), 19.7 ($^1J_{Pt-C}$ = 377 Hz, Pt−*C*H$_2$=*C*H$_2$), 13.9, 13.2, 12.4, 11.6 (2C, 1C, 2C, 1C, Tp′*C*H$_3$), −16.0 ($^1J_{Pt-C}$ = 625 Hz, Pt−*C*H$_3$). ^{11}B NMR (THF-d_8, δ): −8.72. Anal. Calcd for $C_{18}H_{29}N_6BPt$: C, 40.38; H, 5.46; N, 15.70. Found: C, 40.09; H, 5.38; N, 15.45.

Tp′Pt(C$_6$H$_5$)(NCCH$_3$) (15). A 0.100 g amount of Tp′Pt(C$_6$H$_5$)$_2$H (0.15 mmol), 0.03 mL of HBF_4·Et_2O, 2 mL of CH_3CN, and 12 mg of NaH (0.50 mmol) were combined as described above. Yield: 20 mg (21%). IR (KBr): ν_{BH} = 2474 cm^{-1}. ^{1}H NMR (CD_2Cl_2, δ): 6.88, 6.82 (m, 5H, Pt−C$_6$*H*$_5$), 5.94, 5.76, 5.75 (s, 1H each, Tp′C*H*), 2.44, 2.39, 2.38, 2.27, 1.76, 1.48 (s, 3H each, Tp′C*H*$_3$ and Pt−NCC*H*$_3$). ^{13}C NMR (CD_2Cl_2, δ): 150.4, 149.3, 147.4, 146.4, 146.0, 142.7 (Tp′*C*CH$_3$), 137.4, 126.5, 123.0 (Pt−*C*$_6$H$_5$), 115.1 (Pt−N*C*CH$_3$), 106.7, 106.4, 105.9 (Tp′*C*H), 14.9, 13.9, 13.87, 13.8, 13.1, 11.5 (Tp′*C*H$_3$), 4.2 (Pt−NC*C*H$_3$). Anal. Calcd for $C_{23}H_{30}N_7BPt$: C, 45.25; H, 4.95; N, 16.06. Found: C, 45.42; H, 5.07; N, 15.77.

X-ray Crystallography. Single crystals of **3**, **6**−**9**, and **12** were each mounted on a glass wand and coated with epoxy in order to collect structural data,. Diffraction data were collected on a Bruker SMART diffractometer using the ω-scan mode Complete details are given in Table 9.

Acknowledgment. We gratefully acknowledge the Department of Energy (Grant No. DE-FG02-96ER) and the National Institutes of Health (Grant GM 28938) for support of this research. We wish to thank Dr. David Harris for assistance in the ^{11}B NMR measurements.

Supporting Information Available: Complete crystallographic data, in CIF format, for **3**, **6**−**9**, and **12**. This material is available free of charge via the Internet at http://pubs.acs.org.

OM000440Z